Soft Materials

ISSN: (Print) (Online) Journal homepage: https://www.tandfonline.com/loi/lsfm20

A review on graphene-based materials for removal of toxic pollutants from wastewater

Anitha Kommu & Jayant K. Singh

To cite this article: Anitha Kommu & Jayant K. Singh (2020) A review on graphene-based materials for removal of toxic pollutants from wastewater, Soft Materials, 18:2-3, 297-322, DOI: 10.1080/1539445X.2020.1739710

To link to this article: https://doi.org/10.1080/1539445X.2020.1739710

SOFT MATERIALS
2020, VOL. 18, NOS. 2–3, 297–322
https://doi.org/10.1080/1539445X.2020.1739710

Taylor & Francis
Taylor & Francis Group

A review on graphene-based materials for removal of toxic pollutants from wastewater

Anitha Kommu[a] and Jayant K. Singh[b]

[a]Department of Geological Sciences, University of Texas, El Paso, Texas, USA; [b]Department of Chemical Engineering, Indian Institute of Technology Kanpur, Kanpur, India

ABSTRACT

Graphene, a two-dimensional nanomaterial, is a promising material for desalination and purification of organic and inorganic pollutants in the aqueous system. This review illustrates recent advancement and development using molecular dynamics simulations on graphene-based materials, including graphene and derivatives such as graphene oxide, for water purification applications. To this end, we discuss the performance of graphene-based materials for removing various water pollutants from aqueous media, such as salt, metallic ions, anions, and organic chemicals. This article is envisaged to be valuable for readers to understand the design and performance of various graphene-based membranes as the key components for the next-generation membrane technologies.

ARTICLE HISTORY
Received 1 January 2020
Accepted 2 March 2020

KEYWORDS
Molecular simulations; graphene based materials; organic and inorganic pollutants; adsorption; separation; electric field and external pressure; waste water

Introduction

Rapid industrial development, with growing world population, intensification of agriculture and urbanization, is continuously increasing the contamination of air, water, soil, and aquatic ecosystems which has made it a primary focus of political and scientific attention.[1] The contaminants discharged from the industrial process, agricultural practices, and synthetic chemicals, such as pharmaceuticals and cosmetics, can have significant effects on the eco-environment and threat to human beings and animals.[2,3] Some vast pollutants derived from many industries such as metallurgical, mining, chemical manufacturing, and battery manufacturing industries include toxic heavy metal such as copper, arsenic, lead, cadmium, mercury, nickel, cobalt, toxic gases (NOx, SOx, CO, NH_3), organic compounds (dyes, pesticides, pharmaceuticals), and bio-toxics.[4–8] The dumping of untreated wastewater into rivers, lakes, and other freshwater bodies and their acute exposure poses serious health hazards for humans, and survival of aquatic organisms and living environment.[9,10] The harmful effects of organic dyes and heavy metal ions are numerous such as increased heart rate, bio-accumulative, carcinogenic, paralysis, and even death[11–15] in some cases. Thus, it is necessarily urgent to eliminate the organic and inorganic materials from the industrial effluents before it is released into the environment. Extraction of toxic gases and removal of aqueous pollutants safely and effectively are technically challenging. Several traditional methods are being used for the elimination of hazardous pollutants, which include chemical precipitation, membrane filtration, sorption, ion exchange, electrochemical techniques, and solvent extraction technologies, and ultrafiltration. However, these techniques have some inherent advantages and disadvantages. For example, the disadvantages of these methods are: low removal efficiencies, limited adsorption capacity, high cost, small selectivity, long equilibrium time, and generation of other waste products. One of the challenges in this area is to decrease the energy requirement and infrastructure cost of existing technologies. Thus, it is warranted to develop advanced purification technologies taking advantage of new materials to improve the removal efficiencies of organic and inorganic pollutants from wastewater with minimum energy and cost. This review presents recent molecular dynamics studies conducted on graphene-based materials that are very promising for purification and desalination technologies.

Applications Using Graphene Membranes

Membrane science and technology plays a significant role in chemical and environmental industries with a wide range of applications.[16] In general, desalination is the process of removing organic and inorganic pollutants from wastewater to obtain clean and potable water. Membrane-based desalination techniques, using reverse osmosis (RO) method, are currently considered as more environmentally friendly and energy-efficient than that of thermal desalination methods such as

CONTACT Jayant K. Singh jayantks@iitk.ac.in Department of Chemical Engineering, Indian Institute of Technology Kanpur, UP, 208016, India.

multistage flash and multiple-effect distillation.[17] However, these technologies suffer from low desalination capacity, high capital costs, require large amounts of energy, and have low flux permeation rates.[18–21] The conventional polymeric membranes currently used in RO plants have dominated the global membrane market, such as desalination, water purification, and gas separation due to its simplicity, ease of operation, low cost, and energy efficiency. However, polymeric membranes used in RO plants are prone to fouling, suffer from flux decline under high pressure, undergo rapid degradation, have a low tolerance to high temperature, acids/alkaline, chlorine, organic solvents[22], and does not have high permeability and selectivity (see Fig. 1). Hence, there is a pressing need for the development of novel membranes with high-water permeability coupled with high salt rejection capacity[23,24], which can reduce the energy consumption of the RO process. The ideal membranes should provide high flux and good ion selectivity, improved stability, and resistance to chlorine and fouling. Additionally, it should be fabricated as thin as possible and mechanically robust to maximize permeability, should be chemically inert, must retain a high salt rejection rate throughout its service life, and more porous support layers higher than that of present RO membranes.[25–27] Recently, nanostructures such as zeolites, metal-organic frameworks, and ceramics materials are successfully replaced by the polymeric membranes due to their excellent chemical resistance, high flux, and high rejection rates.[23,28] However, these membrane materials suffer from some limitations such as very brittle under high pressure, manufacturing cost, reproducibility, and defect formation[29] which limits their practical applications in membrane technologies. In this direction, in recent years, carbon-based materials have attracted great interest in their easy accessibility, excellent mechanical properties, biocompatibility, as well as environmental friendliness.[30,31]

Initially, carbon nanotubes (CNTs) were believed to be promising candidate materials for membrane due to their unique hollow structure with open ends and extremely strong mechanical properties.[32,33] However, it is still challenging to synthesize vertically aligned and high-density CNTs with large lengths and low defects.[34] The costs and operational issues have greatly hindered the development and integration of CNTs into large-area membranes.[35] Thus, CNTs remain an active area of research for membrane technologies. In recent years, graphene-based materials have attracted great interest in their potential use in desalination and purification of contaminated water. Graphene, possessing a single-atom-thick sheet of sp^2 hybridized carbon atoms arrayed in a honeycomb pattern, opened a new door for researchers and scholars to fabricate the novel membranes with improved separation capabilities.[36] Potential advantages of graphene include excellent structural, thermal, mechanical, and electronic properties, high-surface functionality, and large surface area.[37,38] With its outstanding properties, graphene shows excellent potential in several applications such as transistor fabrication, supercapacitors[39], improved batteries[40,41], solar cells[42], water purification, atomic permeation, water transportation, and gas separation.[43–45] One such potential application is the use of graphene sheets

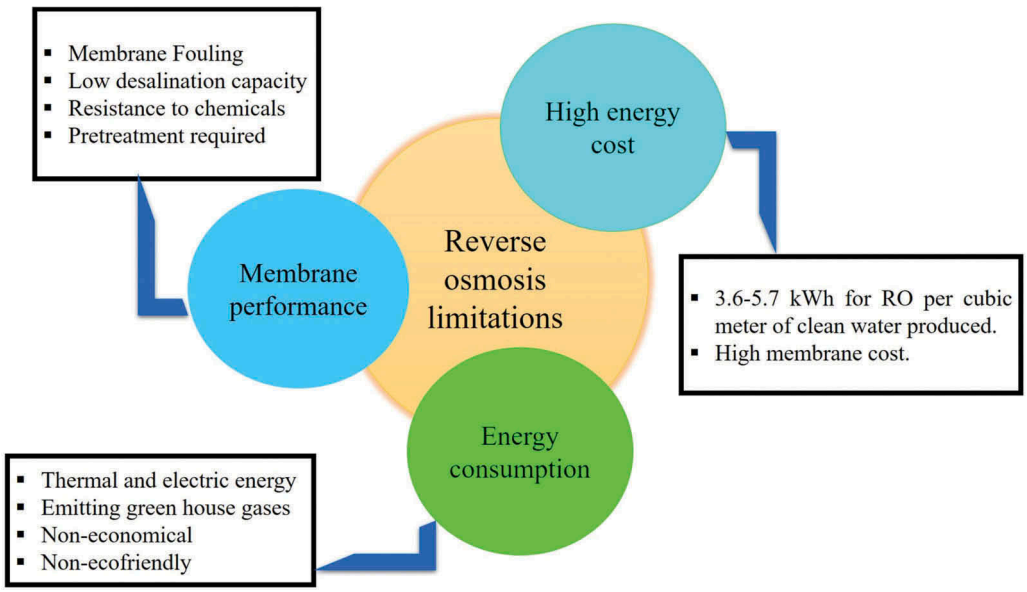

Figure 1. The limitations of classical RO membranes.

as membranes for the separation of undesired components from gases and liquids. Despite its negligible thickness, membranes made of graphene used in the water desalination because they show adequate mechanical strength, capability of functioning under higher pressures, low fouling, high chemical resistance, high selectivity, and fast molecular transport.[21,46] One approach taken by researchers is to create suitable nanopores in graphene sheets. Nanopores in graphene sheet are formed by 'knocking out' carbon atoms from the matrix, which is initially examined through a series of theoretical studies.[47,48] In this section, we present a brief overview of computer simulations and theoretical models developed to investigate gas and water transport through different types of nanoporous graphene (NPG) membranes.

Molecular dynamics simulations are envisaged to provide necessary insight into separation of ions from the aqueous media, and thus providing necessary information for augmenting the designs of RO membranes. To this end, numerous works have been done in recent years using porous graphene membranes for separation of impurities from aqueous media, such as selective ion transport and seawater desalination. We categorize the work done by various researchers into the following sections:

Effect of Pore Size and Doping

Figure 2a shows a typical design of nanopores on graphene sheet[49], with nitrogens, fluorines, and hydrogen functional groups. The functionalized graphene nanopores serve as ionic sieves for high selectivity and transparency. Konatham et al.[50] studied the effect of functionalization of the pores with carboxylated, aminated, and hydroxylated pores on the NPG membranes on its ability to reject NaCl. (see Fig. 2b). It was found that hydroxylated pores gave promising results for the separation of Cl^- ions even at low (0.025 M) and moderate (0.25 M) ionic strengths due to strong free energy barriers for ions passage. However, the selectivity of charged functionalized pores of NPG membranes decreases significantly with increasing ionic strength.

In addition, He et al.[51] simulated using three different functionalized graphene nanopores, namely, four carbonyl(4CO), four carboxylate(4COO), and three carboxylate(3COO) groups, respectively (see Fig. 3a). They found that nanopores containing 4CO preferentially conduct K^+ over Na^+. On the other hand, the 4COO negatively charged nanopore selectivity binds Na+ and transports K^+ and Na^+. The 3COO nanopores with smaller diameter can be tuned by changing the magnitude of the applied

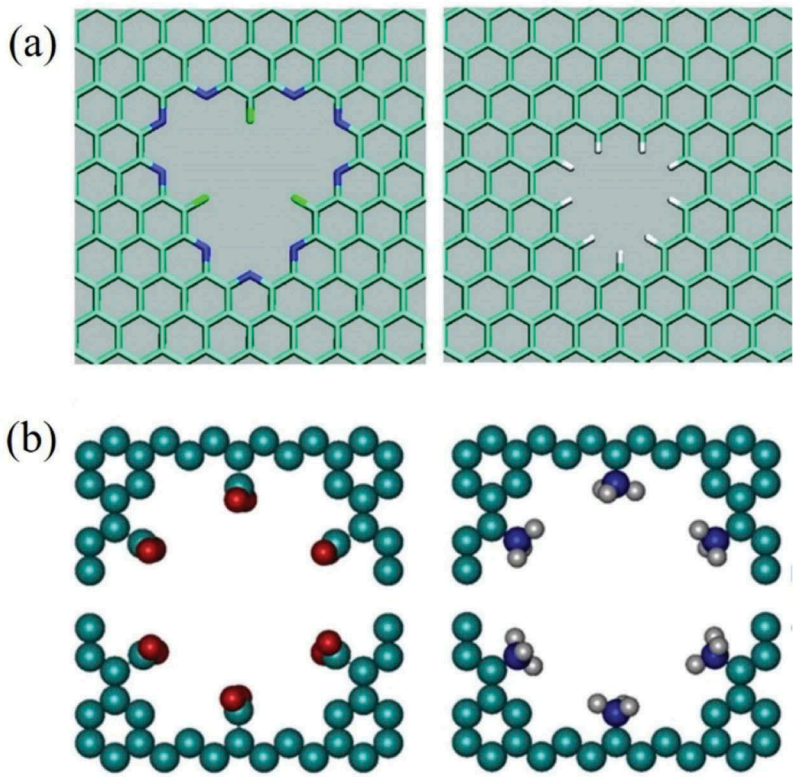

Figure 2. (a) Functionalized graphene nanopores with F–N-terminated nanopore and H-terminated nanopore. Adapted with permission from ref.[49] Copyright (2008) American chemical society (b) Graphene pore functionalized with COO^- and NH^{3+} groups. Adapted with permission from ref[50] Copyright (2013) American chemical society.

voltage bias. Under a lower voltage bias, the passage of Na^+ is favored as a consequence of the selective blockage by Na^+. Under a higher voltage bias, transport of K^+ is favored and Na^+ no longer blocks the pore due to its stronger affinity for carboxylate groups which slows its passage. Various other nanopore configurations[52] for achieving selective permeation are designed by functionalizing the pore rims of nanoporous graphene (NPG) using -H, -F, -OH, etc., as shown in Figure 3b–d. On the other hand, Riyaz et al.[53] investigated the permeability and selectivity using four different sized nanoporous graphene sheet passivated with nitrogen (N) for removal of chromate and arsenate from water. Their work elucidates that the metals ions were physisorbed on the nanoporous graphene sheet surface and they form hydrogen bond between target molecules and nitrogen atoms placed on the edges of the nanopores.

While previous works provide useful insights into how size and chemistry of the nanopores in graphene-based membranes affect their desalination performance, some issues remain open. Recently developed graphene oxide (GO) membranes identified to be excellent candidate materials for filtration and separation applications. GO can be regarded as the oxidized form of graphene having a high density of functional groups containing epoxy, hydroxyl, and carboxyl groups on the surface, and attracted widespread interest due to its exceptional water permeation and molecular sieving properties. Boukhvalov et al.[54], successfully proposed the method and modeling geometries used for the description of graphene–water interfaces and modeling of graphene oxide atomic structure.[55,56] The authors also established atomistic models for hybrid systems composed of water and graphene oxides revealing the anomalous water behavior inside the stacked graphene oxides on the basis of first principles calculations. Joshi et al.[57], performed classical molecular dynamics simulations to support their experimental model and results. They observed in the experimental work that the functionalized GO regions can play a notable role in salt absorption and, more generally, in molecular permeation through GO laminates. They performed MD simulations by setting up the GO by adding 12 hydroxyl and epoxy groups to both walls of graphene capillaries. The results confirmed that smaller ions permeate through the membranes are faster and prefer to reside more time inside capillaries, in agreement with experiments. Most recently, Abraham et al.[58], performed molecular dynamics simulations to evaluate the energy

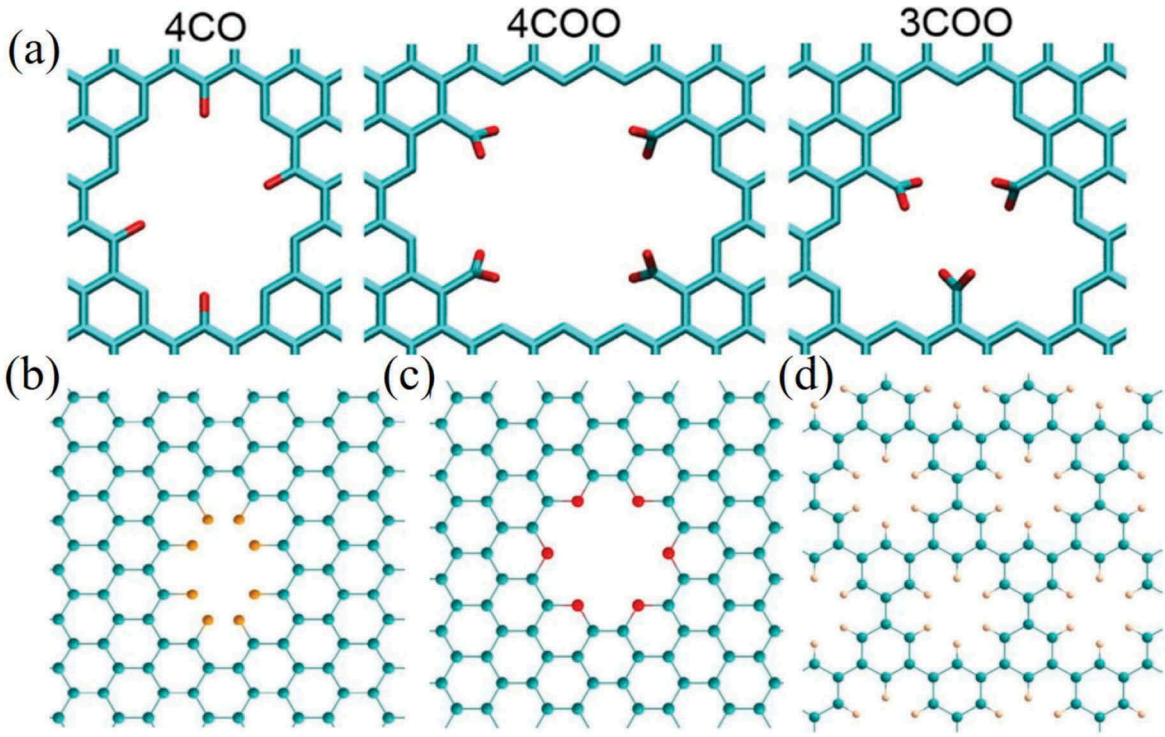

Figure 3. (a) Graphene nanopores functionalized with 4CO, 4COO, and 3COO nanopores are modified with four carbonyl, four carboxylate, and three carboxylate groups, respectively. Adapted with permission from ref[51] Copyright (2013) American chemical society. (b) graphene nanopores passivated using -H, -F, -OH functionalization. (c) Oxygen and nitrogen-based functionalized graphene nanopore (d) stilbene-based nanoporous graphene. (b–d) Adapted with permission from ref[52] Copyright (2018) American chemical society.

barriers for various ions entering graphene capillaries of different widths. The authors revealed that a sharp increase in the energy barrier, for ions, in less than 9Å width of graphene capillaries, which was larger for divalent ions compared with monovalent ions, in agreement with our experiments. Wei et al.[59]explored the water transport in GO membranes by performing atomistic simulations. They elucidate the water flow enhancement inside the nanoconfinement for filtration process, fast water transport through pristine graphene channels breaks down due to a side-pinning effect by water confined within oxidized regions of GO membranes. Guerrero-Avilésa and Orellana[60] showed that the water flux through the hydroxylated pores in close agreement with the experimental report, and found water transport through hydroxylated pores is higher than the hydrogenated pores due to the formation of hydrogen bond between water molecules and O atoms passivated on the graphene nanopore. Recently, Heath et al.[61] studied the molecular interactions between nanopores and alkali atoms and oxygen-passivated graphene nanopores and displayed that binding between alkali and oxygen atoms is strongest when nanopore size is close to the element's van der Waals radius.

Effect of External Pressure and Electric Field

Effect of Applied Pressure

In this section, we discuss the efficacy separating metal ions using NPG membranes and GO membranes, the effect of varying pore diameter, pore chemistry, applied external pressure and electric field. Cohen-Tanugi and Grossman[48] simulated the salt water flow across a variety of pore diameters and chemical functionalization of the NPG membranes (see Fig. 4a), which played an important role in blocking salt ions while passing water molecules through the NPG membranes. Simulation results also show that the transport of water through these nanoporous membranes could reach up to 66 L/cm^2/day/MPa with greater than 99% salt rejection (see Fig. 4b). In contrast, water transport through a conventional RO membrane approximately reaches 0.01–0.05 L/cm^2/day/MPa with a similar salt rejection. Cohen-Tanugi and Grossman also found that water flux through pristine and OH-functionalized pores of the NPG membranes are 2 to 3 times faster than that of the conventional membranes used for reverse osmosis at an equal pressure drop. Nonetheless, the desalination performance of such NPG membranes is most sensitive to pore size, pore chemistry, and applied pressure. The selective rejection of ions through NPG is determined by steric effects, pore size, electrostatic and repulsion interactions between ions and pores, and pore functionalization.[48,49]

As an extension of the initiative research reported by Grossman mentioned above, the effect of pores hydrogenation and hydroxylation on the desalination performance of graphene membranes was further studied by Wang et al.[62] using MD simulations. The authors considered six graphene membranes, with pores terminated with hydrogen (H) and hydroxyl (OH), for desalination performance and systematically investigated the performance of graphene membranes. The water flux and salt rejections were found to depend on both the pore sizes and pore functionalities. The water permeance of 785.6 L/m^2/hr/bar obtained by the authors is two or three orders of magnitude higher than commercially existing technology. Gai et al.[63] calculated the performance of designed graphene pores with ion etching and decorated with negatively charged atoms like fluorine, nitrogen, oxygen, and positively charged hydrogen atoms under various conditions utilizing MD simulations. The tuning of the functional groups on the edges of the graphene pore can provide the best permeability, salt rejection, and high ionic strength. The authors also found that pore selectivity was influenced by the electrostatic interactions between the ions and functional groups positioned at the edge of the graphene nanopore.

Most recently Ang et al.[64] studied the free-standing and frozen nanoporous graphene membrane using MD simulations. They attributed that the free-standing nanoporous graphene membrane can provide a higher salt rejection, but lower water flux as compared to frozen membrane. The authors also investigated the performance of slit membranes as compared to a membrane with circular pore (see Fig. 5a). The authors considered membranes with circular pores with a diameter of 0.5 nm and slits with a length of 0.228 nm. The slit containing membrane showed higher water permeation and perfect salt rejection compared to the circular pores membrane. A similar slit containing membrane was also investigated by Muscatello et al.[65], for the permeation of water through stacked graphene layers via nonequilibrium MD simulation (see Fig. 5b). The simulation results reveal that the path traversed by water molecules has a considerable impact on the water permeability. As an extension of the research reported by the above authors, we recently studied the separation of heavy metal ions from wastewater using NPG membranes.[66]

We investigated the heavy metal-ion separation performance using NPG membranes with variable pore size, pore chemistry, and applied hydrostatic pressure. We compared the nitrogen(N), fluorine(F), and hydroxyl (–OH) functionalized graphene nanopores on the ability to reject metal ions in an aqueous media using water permeability, salt rejection, and free-energy profiles. This study reported that the NPG functionalized with N (NPG-N)

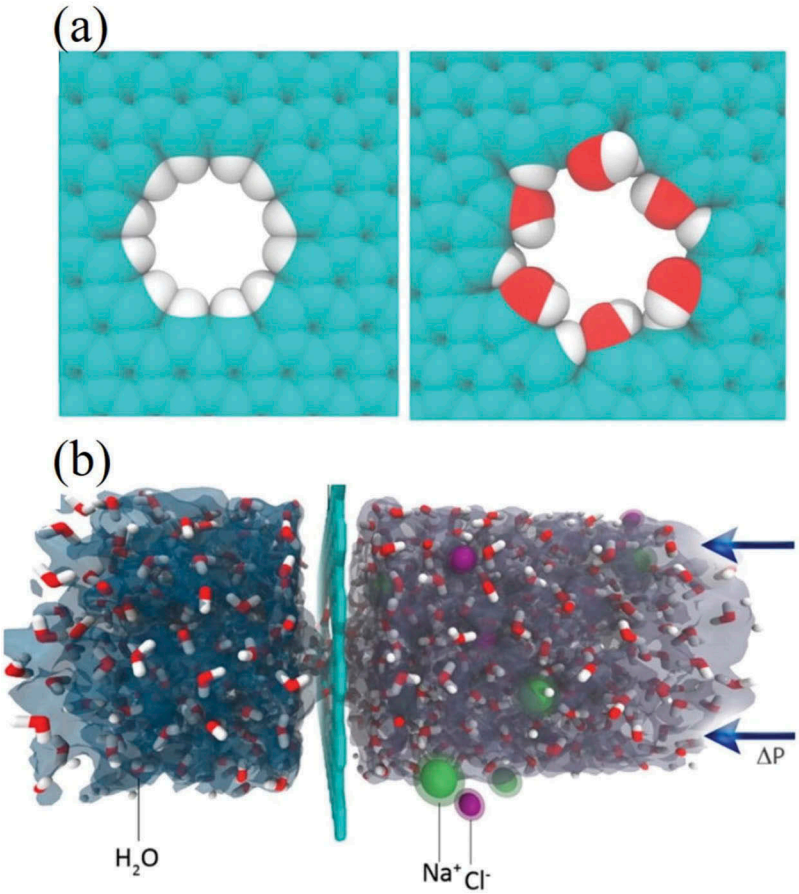

Figure 4. (a) Geometry of hydrogenated and hydroxylated graphene nanopores. (b) side view of the computational system. (a, b) Adapted with permission from ref.[48] Copyright (2012) American chemical society.

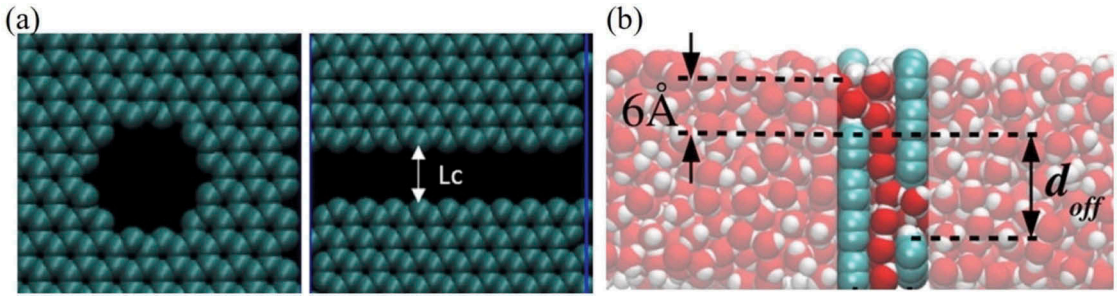

Figure 5. (a) Circular pores A40 of free-standing graphene nanopore membrane and slit-shaped graphene membrane, where Lc is critical slit length. Adapted with permission from ref.[64] Copyright (2016) Elsevier. (b) Geometry of the double-layer graphene sheet membrane was simulated. Adapted with permission from ref.[65] Copyright (2016) American chemical society.

shows higher salt rejection with intermediate permeability compared to NPG functionalized with F (NPG-F) and OH (NPG-OH) groups. The NPG-OH shows higher water permeability through the pore with lower salt rejection compared to NPG-N and NPG-F. However, NPG-F shows lowest permeability compared to other two NPGs considered in this study. The energy barrier for the water molecule is higher for NPG-OH followed by NPG-N and NPG-F, which shows that the water flux will be highest for NPG-F among all the NPGs considered in this study (see Fig. 6a). The water flux and Potential mean force (PMF) results obtained for water using MD simulations are also in agreement with the density functional theory(DFT) calculations. Moreover, the permeability of the water is 4–5 orders more than the existing technologies as shown in Figure 6b. For the case of NPG-OH, we observed very high permeability with ~90% salt rejection percentage compared to NPG-N and NPG-F. On the other hand,

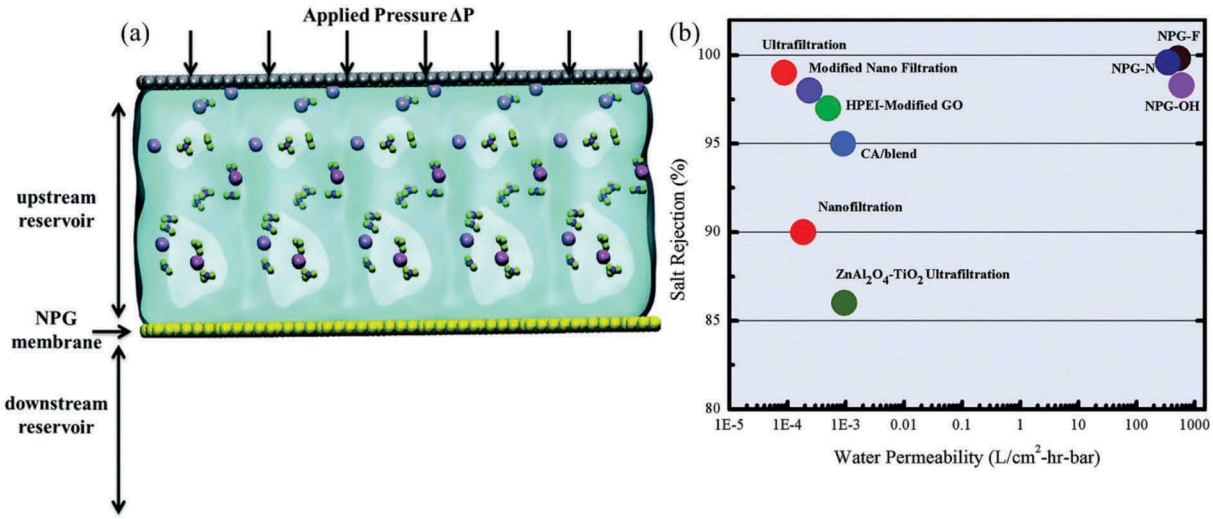

Figure 6. (a) overall view of the computational system, water (light blue surface), metal ions (pink color), nitrate ions (green and red color), and pressure applied on piston (gray color). (b) Comparison of water permeability and salt rejection of functionalized NPG with the existing various technologies reported in the literature. (a–b) Adapted with permission from ref.[66] Copyright (2016) American chemical society.

NPG-N has intermediate permeability with ~100% salt rejection. However, NPG-F shows the low permeability compared to the other two NPGs considered in this study. Overall, the enhanced water permeability and salt rejection using functionalized NPG can offer important advantages over existing technologies.[4,67] The findings thus suggested that ion selectivity can be optimized by varying the pore size, shape, and number of functional ligands attached to the nanopores present in the graphene membrane. While enhancing water flux may not dramatically improve the RO performance because of the thermodynamics limits associated with salt removal, such enhancement is often encouraging because it helps achieve high throughput desalination of water. Other functionalization schemes have also been shown to enable high rejection rate of heavy metal ions and transition-metal ions[66,68] and to more effectively exclude chloride and nitrate ions.[50] Subsequent to the prominent examination of graphene for desalination, numerous theoretical studies have exposed the potential superiority of graphene membranes to state-of-the-art polymer-based filtration.[48,49,66]

Chen and Yang[69] have demonstrated water permeation and salt rejection using monolayer graphene nanopores with pyridinic nitrogen (N) doped functionalization on the pore rims (see Fig. 7a). It was reported that passivation of graphene membranes with various nitrogen-atoms doping at the pore edges increases the water flux six times compared with that of pristine graphene membranes. However, this work exhibits higher water permeability with several orders of magnitude higher than polymeric than RO membranes, along with the 100% salt rejection. Recently, Qiu et al.[70], proposed water desalination using nanoporous graphene passivated by SiH_2 and $Si(OH)_2$ functional groups as shown in Figure 7b,c. They predicted that $Si(OH_2)$ pores enhance superior salt rejection than the SiH_2 functional group nanopore due to selective electrostatic interactions of sodium ions. Thus, the ions are attracted toward the pore and block water transfer. Very recently, Köhler[71] and his group demonstrated that ion flocculant in water improves the salt rejection rate through nanoporous membranes. In another study,[72] Chogani et al. explored the effects of functional groups (methyl, ethyl, and a combination of fluorine and hydrogen) passivated on single-layer nanoporous graphene membrane in water desalination process using MD simulations. Results revealed a suitable distribution of alkyl functional groups is efficient.

So far only computational results were discussed. For graphene nanoporous membrane, enormous effort has been made by the scientific community to bring this concept to experimental verification. However, due to the difficulty in generating precise and uniform sub-nanometer pores, there has been limited success. We discuss here the successes in the experimental realization and testing of nanoporous graphene membranes, as well as the limitations, and challenges, are discussed in length. In 2015, Surwade et al.[73] reported experimentally the effective desalination with KCl solution through the nanoporous graphene membrane, by measuring extremely low ionic transport but measurable water transport. Oxygen plasma etching technique is used for creating nanopores on graphene sheet and achieved a salt rejection of about 76% at high

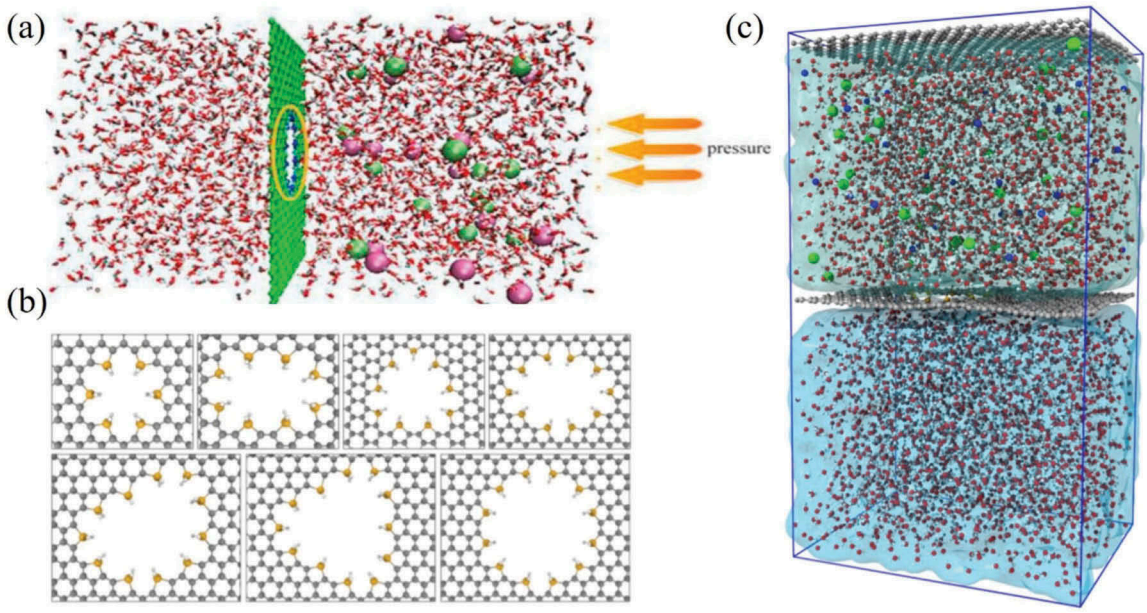

Figure 7. (a) Lateral view of the simulation system, showing a functionalized graphene membrane placed in the center of the box and two chambers on both the sides of the functionalized graphene. The right chamber contained NaCl solution, while the left chamber was pure water. Adapted with permission from ref.[69] Copyright (2015) Elsevier (b) Silicon-passivated nanopore models. Top row: Si-6, Si-8, Si-9, Si-10. Bottom row: Si-11, Si-12, Si-12 s. (c) Simulated system in 3D periodic boundary conditions. Top half represents the feed side (green surface) and bottom half represents permeate side (blue surface). Particles: Green – Cl^-, Blue – Na^+, Grey – C, Yellow – Si, Red – O, White – H. (b, c) Adapted with permission from ref.[70] Copyright (2018) American chemical society.

permeability. More promising results were reported in 2019, by Kazemi et al.[74], where extremely high-water permeation using hydrodynamic pressure was obtained for a large-area single-layer graphene membrane (100-μm scale). In 2017, Qin et al.[75] fabricated a large-area 63 cm^2 graphene nanoporous membrane and reported that membrane shows flux a few times higher as compared to typical polymeric membrane, not able to reject salt ions. The water permeability and salt rejection from computational studies are in agreement with the experimentally measured data and consistent with the continuum theories, as indicated by Wang et al.[76]

In summary, many numerical experiments on nanoporous graphene membrane for sub-nanometer separation operation have illustrated its enormous potential. In particular, the feasibility of nanoporous graphene membranes to perform sub-nanometer separation with high permeability is well established at the lab scale. However, much work is needed to bring the concept to actual industrial applications.

Recently Cohen-Tanugi et al.[77], explored multilayered graphene membranes for water desalination using molecular dynamics, and they found that fully aligned pores and smaller interlayer distances effects water permeation and salt rejection (see Fig. 8a). Yoshida et al.[78] investigated the permeation of water across the multiple graphene layers having nanoslits in a staggered alignment using MD simulations (see Fig. 8c), with an interlayer distance ranging from several angstroms to a few nanometers. The authors compared the results for the water permeability obtained using MD simulations with the predictions obtained using the lattice Boltzmann calculations and hydrodynamic modeling. Dahanayaka et al.[79] investigated the flow across the stacked graphene layers as forward osmosis (FO) membranes by using molecular dynamics simulations as shown in Figure 8b. The optimum layer separation distance between stacked graphene membranes, the larger pore widths, and completely misaligned pore configuration can retain the complete ion rejection and maintain a high-water flux. The results from these studies can act as a guide in developing advanced graphene-based thin films for seawater desalination via FO. Many experimental studies have difficulty in controlling pore generation, particularly in multilayered graphene. To date, not many experiments have been performed for multilayer nanoporous graphene membrane, apart from the 2014 bilayer graphene membrane by Celebi et al.[80]

The recent studies of Kargar et al.[81] provided an overview of the behavior of confined water flow inside the nano-capillaries of length 52Å and thickness of

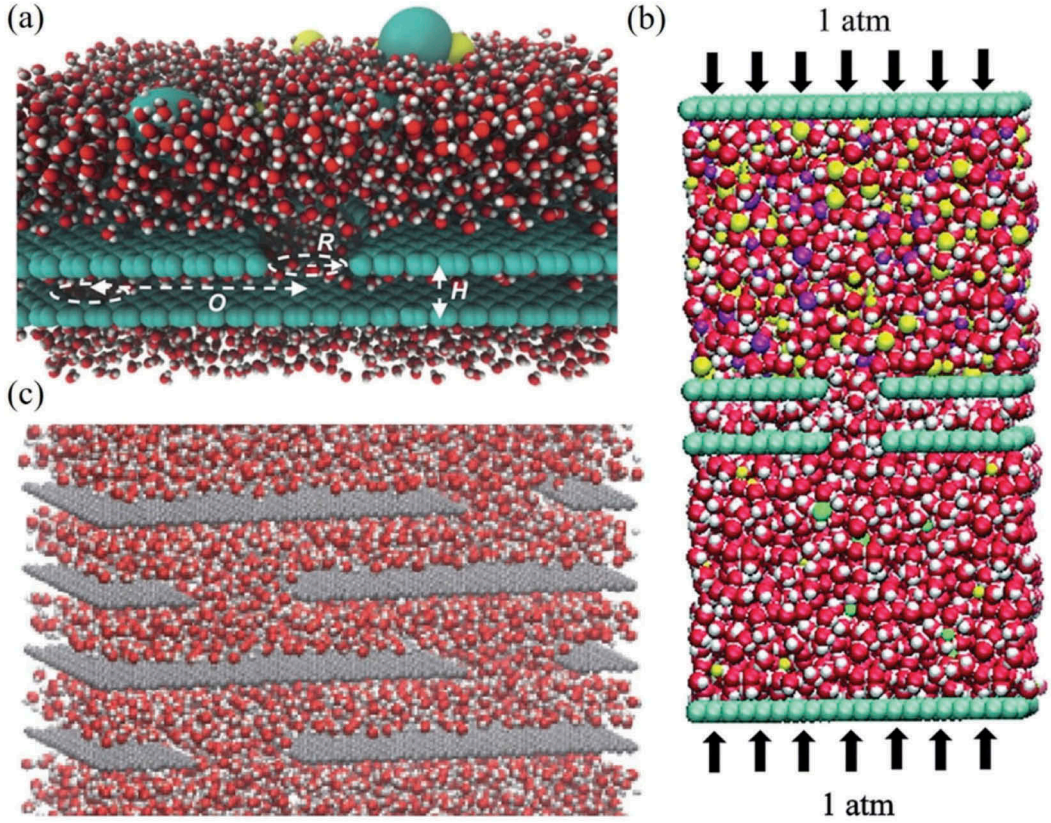

Figure 8. (a) Bilayer membrane with nanopore radius R, layer separation H, and nanopore offset O. Adapted with permission from ref.[77] Copyright (2016) American Chemical Society (b) Schematic representation of the simulation system of the bilayer graphene membrane. Cyan, red, and white color represents carbon, oxygen, and hydrogen atoms, respectively; green, purple, and yellow color represents sodium, magnesium, and chlorine ions, respectively. Adapted with permission from ref.[79] Copyright (2017) Royal society of chemistry (c) A snapshot of the multi-layered graphene membrane. Adapted with permission from ref.[78] Copyright (2016) AIP publishing.

10–15Å, via the application of (MD) simulation method. Their results represented the third-order polynomial variation in the water flow as a function of applied pressure and nanochannels thickness. In addition, the study by Sahu et al.[82] reported that the water permeation and salt rejection through graphene-based membranes are seriously influenced by the parameters such as pore size, applied pressure, and salt concentration. Their results suggested that pore width of 7Å gives 100% salt rejection, and water permeability through this pore width is two order of magnitude higher than the conventional membranes. Seo et al.[83] proposed and fabricated a multilayer graphene slit membrane. The authors reported a high-water flux and salt rejection in line with the reported MD simulations. It is observed that as compared to the nanoporous graphene membrane, the graphene slit membrane is much less explored. However, studies have indicated that it could provide better results, both from the point of view of ease of fabrication and separation performance.

Recently, nanomaterials such as GO membranes show excellent platforms for membrane fabrication primarily due to their ultra-fast water permeation, and mechanical and chemical stability. Few researchers investigated the effect of applied hydrostatic pressure on the ability to remove impurities such as metal ions using nanoporous GO membranes. Nicolaï et al.[84] explored the desalination across as a function of three parameters: linker concentration and thickness of GOF-(n,h) membranes as well as applied pressure ΔP. They showed that the water permeability across GO membranes increases as the pore spacing distance decreases. On the other hand, for a given spacing distance, water permeability increases sharply up to two orders of magnitude higher than the current technologies. Chen et al.[85], performed a pressure-driven flow simulation of ionic aqueous solutions (NaCl, KCl, $MgCl_2$, and $CaCl_2$) across bilayer GO membranes to investigate the effects of staggered nanoslits on desalination properties using MD simulations as shown in Figure 9a. The synthesized flow model divided

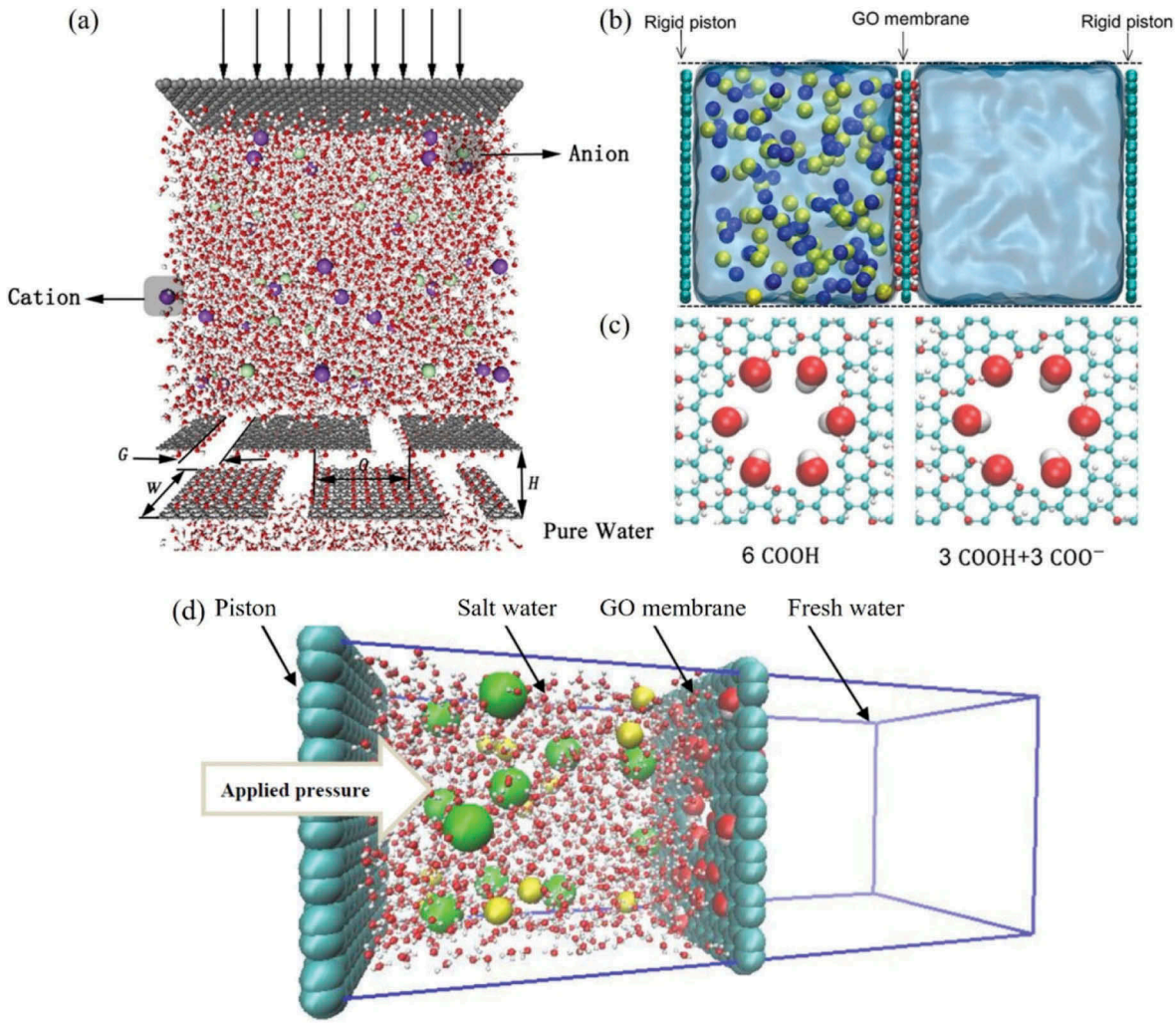

Figure 9. (a) Initial configuration of the simulation system and the geometrical parameters characterizing the GO membrane. The gray, red, white, purple, and lime spheres represent the carbon atoms, oxygen atoms, hydrogen atoms, cations, and anions, respectively. The ball and stick model denotes the saline water molecules and the stick model denotes the pure water molecules. Geometrical parameters *G, O, W*, and *H* stand for the width of gaps, offset between two gaps, width of the laminate, and interlayer spacing distance, respectively. Adapted with permission from ref.[85] Copyright (2017) American chemical society. (b) Representation of the simulation system. The GO membrane has a single nanopore at its center, and six atoms at the perimeter of its pore are functionalized using carboxyl groups. The golden and blue colors denote the Na^+ (Cl^-) ions in the salt water. (c) Zoom-in views of the nanopores in the GO membrane. The red, cyan, and white color denote the oxygen, carbon, and hydrogen atoms, respectively. (b-c) Adapted with permission from ref.[90] Copyright (2017) American Chemical Society. (d) A snapshot of the simulated cell containing a GO membrane for water desalination. The GO membrane placed in the center of box and water molecules and ions added to the one side of the box. (cyan, green, yellow, white, and red colors are carbon, chloride, sodium, hydrogen, and oxygen, respectively). Adapted with permission from ref.[91] Copyright (2012) Elsevier.

into three parts, the entrance of a nanoslit, the conjunction between the gap and passage, and the interlayer inside the capillary channel. It is found that for the same width of the nanoslit, the ability of salt permeation is in the order $K^+ > Na^+ > Mg^{2+} > Ca^{2+}$, which is not consistent with the hydration radii of ions. The permeation of ions through nanoslits and nanocapillaries is not totally up to the hydration radii. Even though the ionic hydration shell is greater than the opening space, the ions can also pass through the split because of the special double-deck hydration structure. These results are useful for evaluating the potential of bilayer GO membranes for the desalination process and it is useful for understanding the transport mechanism of water and salt species across multilayer GO membranes.

Few works[86–89] studied the water permeation and ion rejection in a layer-by-layer assembled free-standing GO membrane. Water permeation across the flexible GO capillary channel is obviously lower than that observed in the channel between pristine graphene

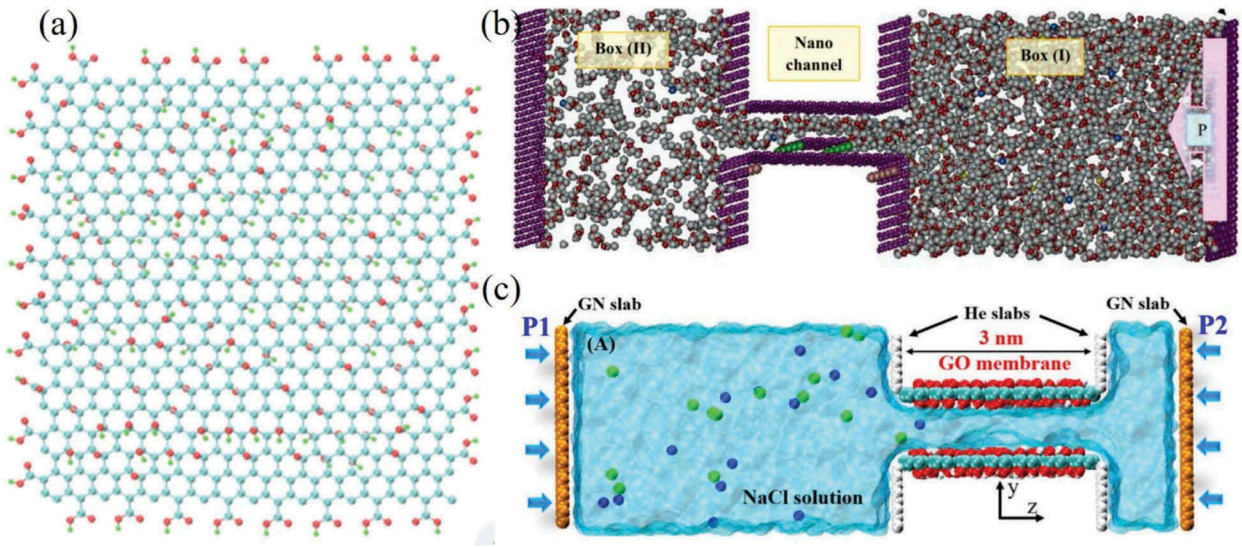

Figure 10. (a) Structure of GO sheet used in the simulation study. Here, red color is for oxygen atoms, green color is for hydrogen atoms and cyan color is for carbon atoms. Adapted with permission from ref.[92] Copyright (2018) Elsevier. (b) The structure of the designed system for model in 3-D view. Adapted with permission from ref.[94] Copyright (2019) Springer Nature. (c) The constructed system used in this study. Blue and green balls represent Na^+ and Cl^- ions, respectively, and water is shown as transparent cyan. Adapted with permission from ref.[95] Copyright (2020) Elsevier.

sheets. Authors demonstrated that the laminate GO membranes with reasonable interlayer distances exhibit high salt rejection ability. The friction coefficient of water flow in the GO channel is two orders of magnitude higher than that for pristine graphene pores, and it increases with the surface oxidation degree. The hydrogen bond interaction between water and functional groups on the GO channel is responsible for the enhanced surface friction.

A recent study by Fang et al.[90] showed how the ionization of the functional groups at the edge of nanopores in single-layer GO membranes affects the desalination efficiency (see Fig. 9b–c). The study reveals that water flux through the pore and salt leakage affected by the ionization of the poresfunctional groups in GO membrane. Moderate ionization greatly enhances water flux and leads to higher salt leakage but too strong ionization reduces the water flux and shows little change in the salt leakage through the nanopores. Ionization of the functionalization groups of the membrane depends on the pH of the feed solution and it has significant effects on the GO membrane's desalination performance. Hosseini et al.[91] performed MD simulations on both nanoporous graphene and GO membranes at the same conditions in order to understand the effects of pore size, pore chemistry and surface functional groups on the water flux, water permeability coefficient, and salt rejection (see Fig. 9d). The results indicated that the hydrophilic groups on the GO membrane showed effective efficiency in salt rejection as well as high performance in water flux. The nanoporous GO membranes allowing water flux 2–5 orders of magnitude greater than other existing reverse osmosis membranes.

Gogoi et al.[92] found that the increasing GO membrane sheet dimension decreases the water permeability; however, the selectivity increases (see Fig. 10a). Water permeation and salt rejection efficiency through GO membranes can be greatly tuned by the pore offset distance of the membranes. The increase in the pore offset distance decreases the permeation of water molecules and increases the ions rejection through the layered GO membranes. Giri et al.[93], carefully investigated the ion permeation, salt rejection, and water structure in GO nanochannels of varying oxidation degree (from 0% to 40%) and varying interlayer spacing (from 0.6 nm to 1.0 nm) via atomistic MD simulations. Their results demonstrated that the water permeation increases with increasing interlayer separation and it decreases with increasing oxidation degree. The results indicated that the best GO channel for the filtration efficiency is for an oxidation degree of 10% or lower and interlayer spacing of 0.8 nm. On the other hand, Lohrasebi and Koslowski[94] studied the transport of water molecules and salt ions through graphene-based nano-channels by changing the parameters such as channel width and charges attached to the channel (see Fig. 10b). Their results indicated that the increased ion rejection and water flow through the nano-channel by enhancing the amount

of charges, and found that the percentage of water flow and selectivity (ion rejection) depends on the geometry and shape of the channel.

The recent work by Qiu et al.[95] showcases water permeability and ion rejection using three typical edge functional groups, namely carboxyl (COOH), hydroxyl (OH), and hydrogen (H) on the GO nanosheets. The resulting high ion rejection rate for COOH edge functional group compared to the OH and H edges functional groups with 7Å interlayer width. The theoretical research related to permeation of water and ion into 2D nanochannels of GO membranes (see Fig. 10c) with different interlayer space and nanostructure have been explored Li et al.[96], using non-equilibrium MD simulations. They showed that the strong electrostatic, vdW, hydrogen bond, and polarization interactions between water/ion and oxygen-containing groups in GO membranes impedes their transport, which greatly can promote the development of desalination membrane using 2D materials with varying interlayer nanostructures.

The Effect of Electric Field

The effect of the external field such as an electric field on the ability to remove impurities such as metal ions using functionalized graphene pores was also investigated by few workers. Azmat et al.[97], in particular, studied the ion removal from the water using two different functionalized graphene nanopores under an external electric field. The results showed that using electric field the functionalized graphene pores by fluoride (F-pore) and hydrogen atoms (H-pore) were permeate, preferentially, the Na^+ and Cl^- ions, respectively. Li et al.[68] simulated the separation performance of $CuCl_2$ from an aqueous solution using nanoporous graphene surfaces as reverse osmosis membranes with three different functionalized groups (boron, nitrogen (N) and hydroxyl (OH) groups). The authors explored the effect of pore chemistry and various conditions on water permeability and ion rejection by computing the interfacial properties and the corresponding potential of mean forces (PMFs) through the three types of functionalized graphene pores. The N-graphene displays the relatively low ion rejection with intermediate permeability. Comparatively, the OH-graphene and boron-doped graphene membrane have displays 100% ion rejection, although the water permeation is lowest for OH-graphene compared to the boron-doped graphene. The simulated water permeability is 2–5 orders of magnitude higher than that of current commercial membranes. The calculations of the potential of mean force revealed that water molecules face lower free-energy barrier as compared with Cu^{2+} ions when passing through graphene pores. The free-energy barriers for Cu^{2+} ion are highest for OH-graphene, followed by boron-doped graphene and N-graphene, correlating well with the observed salt rejection. Overall, the functionalized nanoporous graphene membranes exhibit potential application in the removal of heavy metal ions. In 2016, Rollings et al.-[98] experimentally proved the concept by showing that negatively charged nanoporous graphene membrane with pores as large as 20Å were able to display strong K^+/Cl^- selectivity.

Ruan et al.[99] and Zhu et al.[100] performed molecular dynamics simulations to investigate selectivity behaviors of Mg^{2+} and Li^+ passing through the functionalized graphene nanopore models under various electric field intensities (see Fig. 11a–c). However, graphene-based nanopores are modified with either five carbonyl or five negatively charged carboxylate ions at the edges of the pores for achieving selective permeation of Mg^{2+} ions over Li^+ ions. PMF calculations of ions passing through the functionalized nanopores. This result suggested that the Li^+ ion has a finite energy barrier to pass through both the functionalized graphene nanopores, while Mg^{2+} ions can cross through functionalized nanopores in a barrierless fashion. Moreover, the separation is due to the difference in dehydration behavior between the second hydration shells of Li^+ and Mg^{2+} ions. For Li^+ ions require excess energy for the dehydration compare to the Mg^{2+} ions, and thus shows lower selectivity in permeation of the Li^+ ions over the Mg^{2+} ions.[99,100]

Nguyen et al.[101] reported that transport of saltwater through three different pore sizes of the pristine and positively charged single-layer graphene nanoporous membranes. The positively charged graphene membranes showed that rate of salt rejection is higher compared to the pristine membrane for hydraulic pore diameters of 14.40Å. In addition, Nyguen et al.[102] demonstrated the salt water transport through positively and negatively charged nanoporous graphene membranes with a hydraulic pore diameter of 14.40Å. The results indicate that the nanoporous graphene membranes with four different electric charges distributed on the pore edges show promising performance in reverse osmosis (RO) desalination systems. Zhang et -al.[103] also carried out MD simulations for permeation of salt ions through the graphene bilayer with and without a vertical electric field and found that ions are trapped inside the nanochannels due to the strong electrostatic interactions between them. Lohrasebi and Rikhtehgaran[104]] studied the separation ions through the porous graphene membrane driven by an external electric field and observed ion rejection rates increased

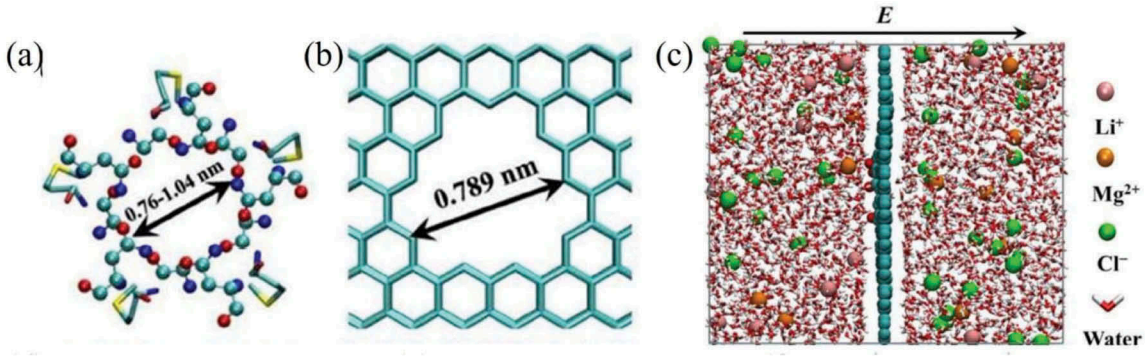

Figure 11. (a) Selectivity filter structure of CorA Mg^{2+} channels viewed from the top. (b) Graphene nanopores with pore diameter of 0.789. (c) The simulation box that consists of a modified graphene nanopore in the center and reservoirs on both sides of the graphene nanopore. (a–c) Adapted with permission from ref.[99] Copyright (2016) American chemical society.

up to 93% for the electric field (E) of 10 mV/Å and higher values of E.

Effect of Functionalization and Grafting

Various molecular simulation studies reveal an important role of terminal groups on graphene-based materials for an enhanced removal of metal ions from aqueous streams.[66,105] The GO can be grafted/functionalized with different polymer groups for the removal of organic and inorganic pollutants from wastewater. Polyamidoamine dendrimers (PAMAMs) are frequently studied due to their large amount of terminal functional groups.[106,107] PAMAM dendrimers are much larger and more versatility in variety of terminal groups, including amino, carboxylic, and hydroxyl groups.

Yuan et al. grafted graphene oxide with dendrimers (GO-PAMAM) has shown a high adsorption capacity of heavy metal ions ~1.0 mmol/gm.[108] Recent experimental work of Zhang et al.[109] explored using GO-PAMAM adsorbent to remove heavy metal ions from aqueous solutions. These experimental investigations showed that the metal-ion adsorption capacity on the GO surface is improved after modification with polymers.

To elucidate the molecular interaction between the metal ions and PAMAM dendrimers, in a recent work[110], we have illustrated the molecular mechanisms involved in the adsorption of metal ions (particularly Pb^{2+}) on the graphene, graphene oxide, and polyamidoamine (PAMAM) dendrimer with different terminal groups grafted on the graphene and graphene oxide surfaces (see Fig. 12a). Using the base materials listed in Table 1, eight different surfaces were generated viz., graphene (GS), GS-PAMAM, GS-PAMAM-COO^-, GS-PAMAM-OH, graphene oxide (GO), GO-PAMAM, GO-PAMAM-COO^-, and GO-PAMAM-OH. An illustration of such a system, using the G3 generation PAMAM dendrimer is shown in Figure 12b,c. Adsorption of Pb^{2+} ions on the GO-PAMAM-COO^- surface is significantly more than the other surfaces for all five concentrations considered in this work as shown in Figure 12d.

The maximum adsorption capacity of GO-PAMAM for Pb^{2+} ion is found to be 568.18 mg/g at around 6 mmol/L. The experimental findings of the order of adsorption of Pb^{2+} metal ion on the different surfaces GO-PAMAM> GO > GS is qualitatively akin to that seen in our work.[109] The maximum adsorption capacities of Pb^{2+} ion on different surfaces calculated from the Langmuir isotherm equation follow the order GO-PAMAM-COO^- > GO-PAMAM-OH> GO-PAMAM > GO > GS-PAMAM-COO^- > GS-PAMAM-OH > GS-PAMAM > GS.

The adsorption capacity of Pb^{2+} ions on the dendrimer grafted on the GO surface is significantly more than the bare GO, bare GS and dendrimer grafted GS surfaces for five concentrations. The adsorption mechanism of metal ions on the eight different surfaces is discussed with the help of microscopic interactions between metal ion and solid surfaces. In addition, we examined the self-diffusion coefficient and residence time of Pb^{2+} ions near the surfaces. Interestingly, we found that the interaction between the Pb^{2+} ion and dendrimer plays a significant role in enhancing their association with the dendrimer grafted surfaces. The results show that the adsorption capacity of the Pb^{2+} ion is improved significantly using carboxyl terminal groups of dendrimer grafted on graphene oxide surface.

Graphene and GO for Removing Organic Pollutants

Among various techniques, the adsorption method is considered to be one of the simplest and most attractive methods for separating organic pollutants from wastewater. The ideal adsorbent material should exhibit high gravimetric

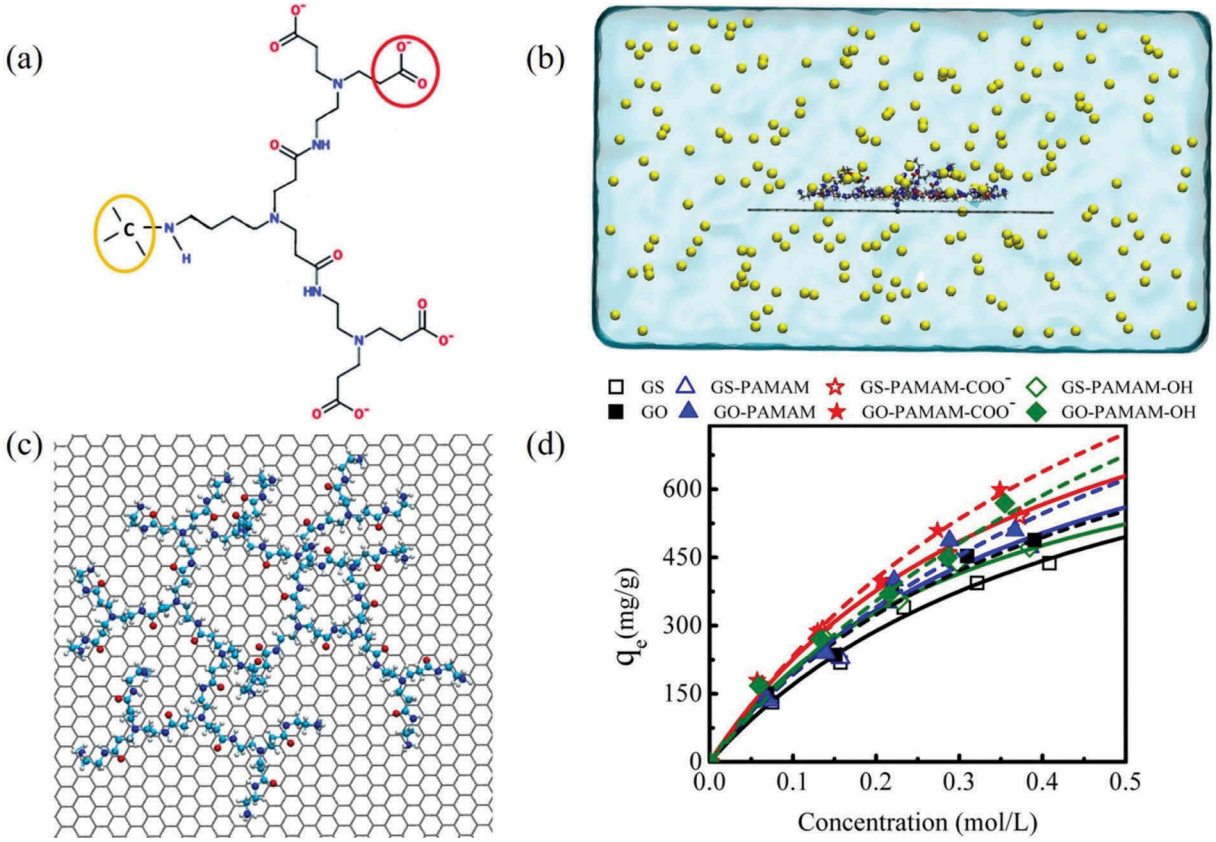

Figure 12. (a) Schematic diagram for a G0.5 PAMAM-COO^- grafted onto graphene sheet where red circle group represents a carboxyl-terminal group and yellow circle represents a carbon atom within the graphene sheet (GS). (b) Representative simulations system GO-PAMAM surface solvated in an ionic solution. Grey color represents the GS, cyan, red, blue, and white colorsrepresent the carbon atoms of PAMAM dendrimer, oxygen atoms of functional groups and PAMAM, nitrogen atoms of PAMAM and hydrogen atoms of functional groups and PAMAM. Water represented as the light blue surface, nitrate ions represented as green and pink, and metal ions as shown in yellow. (c) GO-PAMAM surface. (d) Langmuir adsorption isotherm showing the variation of total amount of metal ion adsorbed (qe) with the concentration (mol/L) for adsorption of Pb^{2+} ions onto the eight different surfaces. Open symbols for different terminal groups (-NH_2, -COO^- and -OH) of dendrimer grafted to GS surface and filled symbols for different terminal groups (-NH_2, -COO^- and -OH) of dendrimer grafted to GO surface. Adapted with permission from ref[110] Copyright (2017) American chemical society.

Table 1. Summary of the materials considered.

Material	Description
GS	Graphene sheet
GO	Graphene oxide
PAMAM	Dendrimer with NH_2 terminal groups
PAMAM-COO^-	Dendrimer with COO^- terminal groups
PAMAM-OH	Dendrimer with OH terminal groups

capacity, easy separation from cleaned water and easy cleaning for long-term cycling. The most common adsorbents are activated carbon[111], zeolites[112] and natural fibers[113], and other recent refined materials, including graphene capsules[114], collagen nanocomposites[115], polyurethane sponge[116], polyurethane, and iron oxide composites[117], MnO2 nanowires[118] and graphene hydrogels.[119] These adsorbents have been used for removal of organic solvents such as alcohols, aromatic compounds, and dyes from aqueous phase. However, these adsorbents have significant disadvantages such as low efficiency, unsatisfactory regeneration, and cycling ability. In this direction, two-dimensional graphene materials have attracted much recent attention because of their unique properties including high-surface area.[37,120] Azamat et al.[121] performed MD simulations to study the separation of chlorination disinfection by-products such as CH_3Cl, CH_2Cl_2, and $CHCl_3$ in aqueous solution using functionalized graphene pores under induced pressure. The graphene pores terminated with fluorine and hydrogen atoms with different pore sizes showed that the functionalized nanoporous graphene with a small diameter is impermeable to trihalomethanes (CH_3Cl, CH_2Cl_2, and $CHCl_3$) whereas larger diameter pores are permeable to trihalomethanes. These results suggest that a thin graphene membrane with a functionalized pore can effectively filter the trihalomethanes from water under pressure.

Zhao et al.[122] studied the effect of pore width and composition of ethanol-water mixtures confined

within slit-shaped graphene nanopores using MD simulations (see Fig. 13a). They found that ethanol molecules were preferentially adsorbed on the inner surface of a pore wall and formed an adsorbed ethanol layer. Essentially, the adsorbed alcohol layer acts like a new surface for water molecules to adsorb on it. The diffusion coefficients for confined pure ethanol molecules are substantially less than that of bulk phase, indicating more enhanced confinement effect as shown in Figure 13c. In our recent work[123], we performed MD simulations to investigate the selectivity of ethanol-water in slit-shaped graphene pores (see Fig. 13b). In particular, we investigated the structural (i.e., density profiles, hydrogen bonding, and molecular orientation) and dynamical properties (i.e., self-diffusion coefficients and residence time) of ethanol-water confined in slit pores. In order to compare the properties of confined water and ethanol molecules within different pore widths of graphene sheets, we considered three pore sizes (7, 9, and 13Å) under identical conditions. The suitability of the sheets for the separation of ethanol-water mixture is investigated by studying the adsorption and structural behavior of ethanol-water mixtures in slit pores with variable width (7 to 13Å) using MD simulations. The selectivity of ethanol is found to depend on the pore-width and nature of the pore walls. The selectivity of ethanol is highest for 9Å pore and lowest for 7Å pore. The investigation of the structural properties of the confined ethanol and water molecules within different pore widths are used to elucidate the adsorption behavior. Results from this study showed that the adsorption of ethanol molecules inside the graphene pore increases with increasing mole fractions of ethanol-water mixture. By comparing the selectivity of ethanol molecules within the different slit pores, 9Å slit pore shows the highest efficiency of ethanol-water separation compared to the 7 and 13Å pores. The combination of structural and dynamical properties results reported here for ethanol-water system suggests that pore size 9Å of graphene surface is useful for the separation of ethanol from ethanol-water system (see Fig. 13d). Based on the above results, it can be concluded that molecular sieving plays an important role

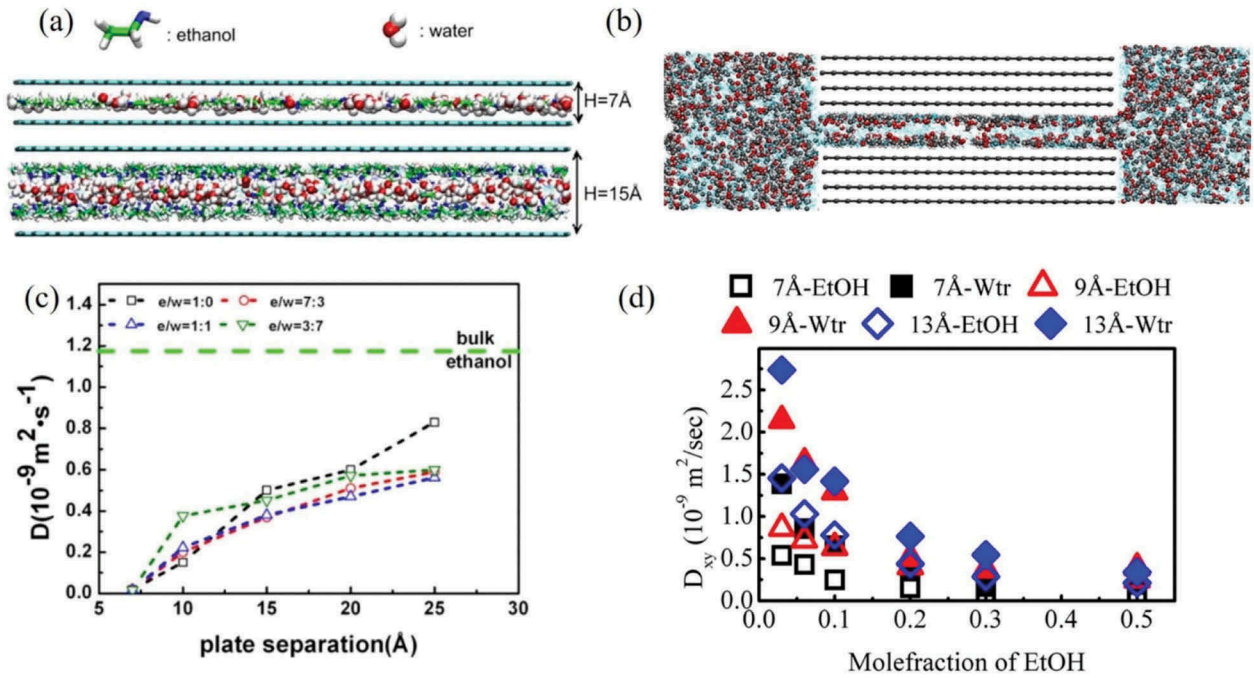

Figure 13. (a) Representative of simulation systems. The cyan walls represent the graphene sheets. Adapted with permission from ref[122] Copyright (2015) American chemical society. (b) Representative simulation snapshot for the water/ethanol mixture in contact with the 13 Å graphene pore. Red and white spheres represent oxygen, hydrogen atoms, and gray spheres represent carbon atoms of ethanol molecules, respectively. Cyan color represents water molecules. Grey color spheres represent the carbon atoms of graphene surface, respectively. Adapted with permission from ref[123] Copyright (2017) American chemical society. (c) Diffusion coefficients of ethanol with various ethanol/water compositions confined in 7–25 Å graphene nanochannels. Diffusion coefficient of ethanol in bulk phase represented by green dash line. Adapted with permission from ref[122] Copyright (2015) American chemical society. (d) Diffusion coefficient for water and ethanol molecules within three slit-shaped pores on the graphene (GS) surface as a function of ethanol mole fraction. Adapted with permission from ref[123] Copyright (2017) American chemical society.

in lower pores, whereas surface-fluid interaction is a governing factor for larger pore sizes.

In a recent work, Joshi et al.[57] using MD simulations have confirmed that the graphene-based materials with well-defined pore sizes can be used for filtration and separation technologies for the extraction of valuable solutes from complex mixtures. The graphene capillary acts as molecular sieves, blocking all solutes with hydrated radii larger than the capillary size. Results show that the selectivity of ethanol decreases with increase in mole fraction of ethanol. The selectivity of ethanol is higher for 9Å slit pore compared to 7 and 13Å pores. The results confirm that the ethanol molecules easily permeate through the 9Å slit pore compared to the 7Å. However, the ethanol molecules transport into the graphene pores obviously depend on the width of the pore. Therefore, the pore width is the crucial parameter to dictate the selectivity of ethanol. This suggests that pore 9Å of graphene surface is promising for ethanol/water separation. The above studies focused on the preferentially adsorbed ethanol molecules on the inner surface of the pore wall and also the mobility of water molecules under 2D nanoconfinement. Gao et al.[124] investigated the effect of the alcohol adsorption layer on the mobility of water molecules under 2D confinement. Molecular simulations were performed to evaluate four types of alcohol/water binary mixtures confined under a 20Å graphene slit. The alcohol/water binary mixture separation under 2D graphene slit is usually affected by multiple factors, such as pore size, pore wall chemistry, and external conditions, respectively. They found that residence times of the water molecules covering the alcohol layer were in the order of methanol/water < ethanol/water <1-propanol/water < 1-butanol/water. The authors analyzed the hydrogen bonding (H-bond) network between the preferentially adsorbed alcohol molecules and the surrounding water molecules. They observed a low average number of H-bonds, which could be due to the damage of H-bond network of the water molecules covering the alcohol layer, resulting in the long residence time of the water molecules.

Recently, Borges et al.[89] investigated the molecular level mechanism for the separation of alcohol/water inside multilayer GO membranes. The authors explained the selectivity of water in nano-confined structures and effective blocking of alcohol molecules by performing deep analysis on the structural molecule arrangements inside GO channels and the water permeation mechanisms using molecular simulations. They found that both the size exclusion and molecular arrangements within GO channels are responsible for the separation of alcohol/water and this is due to the formation of water monolayer is enhanced by the formation of a robust hydrogen bond network. It was found that the key factors for designing more efficient alcohol-water separation membranes are permeability, membrane affinity, molecular size exclusion, and geometry confinement, respectively. They suggested that GO membranes are versatile and efficient for ethanol dehydration using this separation process. Borthakur et al.[125] studied the influence of different inorganic anions (Cl^-, Br^-, SCN^-, NO_3^-, $SO^4{}_2^-$ and CH_3COO^-) and cations (Ca^{2+}, Mg^{2+}, Na^+, and NH_4^+) on the surface potential of GO suspension using MD simulations. The simulations are performed by solvating single GO molecule in both acidic and basic forms in pure water and aqueous solutions of NaCl, Na_2SO_4, NaSCN, $NaNO_3$, NaBr, CH3COONa, NH_4Cl, $MgCl_2$, and $CaCl_2$ with the 0.1 M concentration. The results from MD simulations suggested that the interactions between cations and anions with the surface of GO and correlate to the measured zeta potential to the presence of inorganic ions in the colloidal suspension at molecular level. This work showed that GO successfully utilized in the reactive extraction technique for separation of methyl blue dye molecule from aqueous phase to organic phase. Hou et -al.[126] demonstrated the adsorption behavior of calcium and sulfate ions on four different types of surfaces such as graphene sheet (G), GO with carboxylate (GOCOO–, deprotonated carboxyl), GO with carboxyl (GOCOOH) and GO with hydroxyl (GOOH). They found that the adsorption of calcium and sulfate ions is greatly depended on the polarity of GO surface, and consequently adsorption ratio follows the order: $GOCOO^-$ > GOCOOH > GOH> G.

GOs are two-dimensional one-atom-thick nanosheets with a large surface area that can facilitate drug adsorption on their surfaces and edges through mechanisms such as π-π stacking, electrostatic interactions, and hydrogen bonding. Therefore, the drug loading capacity of GO is typically larger than other nanoparticle-based carriers. Wang et al.[127] and Mahdavi et al.[128] have investigated, independently, a graphene-based drug delivery system for DOX and three other anticancer drugs, i.e., chlorin e6 (Ce6), MTX, and SN38. They specifically focused on the effect of graphene sheet size on the drug diffusion and adsorption on the pristine graphene (PG), GO, and polyethylene glycolfunctionalized GO (GO-PEG) in vacuum. They conclude that the drug adsorption is more favorable when the drug molecules and graphene nanosheets become comparable in size. Moreover, the drug molecules interact more strongly with the GO-PEG carrier than with the PG sheets, which highlights the advantages of functionalization in improving the stability of graphene-based drug

delivery systems. Previous research has not adequately explained the underlying mechanism of DOX adsorption on graphene-based nanocarriers in an aqueous medium at different pH levels. Mahdavi et al.[128] studied the adsorption of doxorubicin (DOX) anticancer drug on pristine graphene and graphene oxide nanocarriers, with different surface oxygen densities, in an aqueous environment with varying pH levels using MD simulation (see Fig. 14a). They revealed the underlying mechanisms of DOX loading and release on graphene and GO surfaces, which would be valuable to design better graphene-based nanocarriers for the DOX delivery and targeting applications. The authors demonstrated that there exists a significant difference in the adsorption of multiple DOX molecules on a GO sheet at neutral versus acidic pH levels. Thus, the simulation results can be used to design suitable DOX/GO drug delivery systems with desirable pH-induced drug release characteristics. Moreover, the GO could be used as a potential nanocarrier for the delivery of other anticancer drugs, such as camptothecin and paclitaxel.

Safdari et al.[129] analyzed the adsorption behaviors of the 5-fluorouracil (5-FU) anticancer drug on the surface of graphene oxide nanosheet using DFT and MD simulation. The geometrical, topological, and electronic properties of 5-FU molecule adsorption on the GO nanosheet are employed using DFT calculations. Moreover, the authors also investigated the effect of temperature (250, 300, 350, and 400 K) on the dynamic interaction between GO nanosheet and 5-FU drug molecules in an aqueous environment using MD simulations. The results obtained from MD simulations illustrate that the increasing temperature to 400 K promotes the hydrogen bonds between different functional groups on GO nanosheet and 5-FU drug molecules. It is also found that by increasing the temperature from 250 to 400 K, the van der Waals interaction energy of the simulation system becomes more negative. Recently Hasanzade et al.[130] studied the adsorption of ellipticine (EPT) drug on the surface of graphene oxide

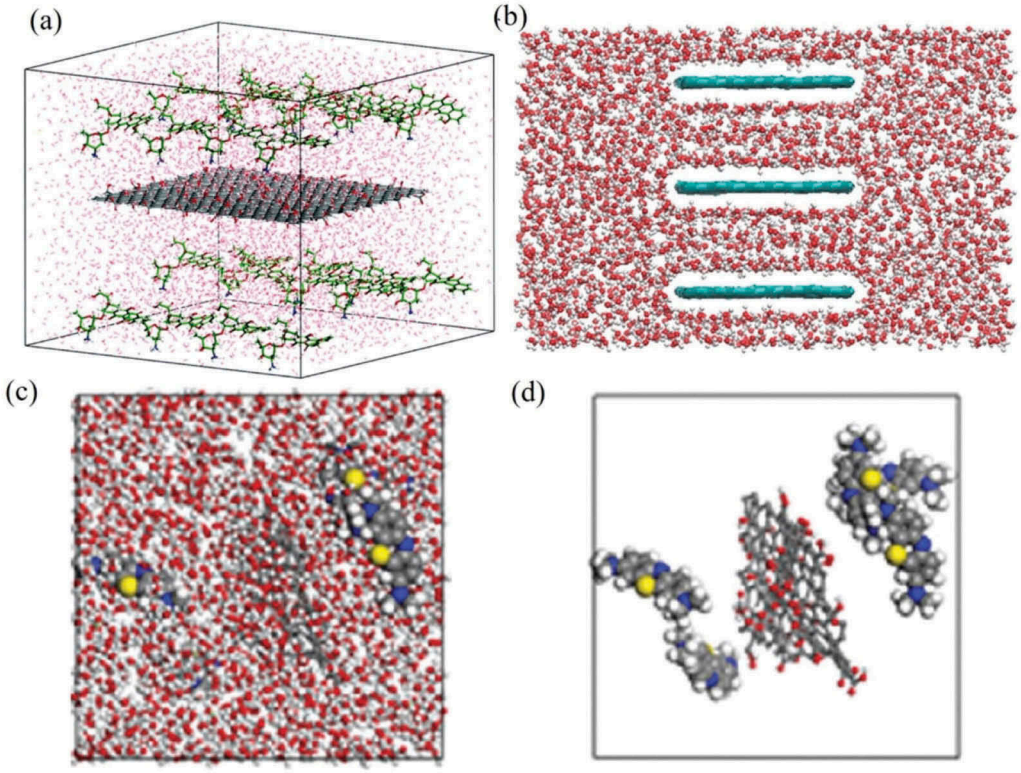

Figure 14. (a) Adsorption of doxorubicin (DOX) drug molecules on GO graphene oxide at pH = 7. Adapted with permission from ref[128] Copyright (2016) Royal Society of Chemistry (b) GO membrane models with d_{eff} = 10.19 Å after capillary filling. The red, and white color denote the oxygen, and hydrogen atoms of water molecules. Adapted with permission from ref[135] Copyright (2016) American chemical society. (c) Representative simulated system for adsorption of methylene blue cations on GO in an aqueous solution. (d) Zoom-in views of the methylene blue cations and GO solvated in an aqueous solution. Water molecules are not shown for clarity. The color of atom represents the following rule: white, hydrogen; red, oxygen; gray, carbon; blue, nitrogen; yellow, sulfur. The GO is shown as gray–bonded sheet, while methylene blue cations are shown as larger spheres. (c-d) Adapted with permission from ref[134] Copyright (2015) AIP publishing.

nanosheet using density functional theory and molecular dynamics simulations. They examined the effect of the pH on the drug molecule loading and released on GO nanosheet. MD simulations results showed that the favorable drug molecule loading at the neutral blood pH level and its release at an acidic pH level of the environment surrounding a cancerous tumor. The results from this study explain the molecular mechanisms of EPT loading and release under the influence of pH, which is useful for development of a pH-controlled drug delivery system using GO carriers.

Tang et al.[131] studied the adsorption of aromatic compounds on GO by combining MD simulations, and DFT calculations. The authors studied the adsorption capacity of aromatic compounds on GO governed by the π-stacking ability, polarizability, and hydrogen bond interaction energy. You et al.[132] investigated the adsorption action of nonylphenol ethoxylates ($NPEO_{10}$) on GO surface, where theoretical calculation from MD simulation demonstrated that the adsorption capacity mainly depends on the polar interactions between the ethoxylate group and oxygen-containing functional group on the GO surface. In a recent work[133], molecular dynamics simulations were conducted to study the adsorption of three different types of dye molecules (i.e. methylene blue (MB), rhodamine B (RhB) and methyl orange (MO)) on GO surface. The calculated adsorption energies elucidate electrostatic interactions between the dye and the GO model. The study illustrated that GO has better adsorption of cationic dyes (MB and RhB) compared to the anionic dyes (MO). Liu et al.[134] performed MD simulations to understand the molecular mechanism interactions between the GO sheet and methyl blue (MB). This study revealed that the GO can remove almost all MB from aqueous solutions due to the strong electrostatic interactions between GO and MB molecular. The MD simulations showed that the MB cations quickly congregate around GO in an aqueous solution as shown in Figure 14c,d. The effective removal of radioactive technetium from contaminated water is of enormous importance from an environmental and public health perspective. Williams et al.[135] demonstrated that GO membrane capillaries are used for removal of technetium from water using molecular dynamics simulations as shown in Figure 14b. PMF of individual anions are calculated when entering into the membrane capillaries. They also investigated the effect of changing the capillary diameter and observed the entrance barriers of anions using PMF calculations. The results from this study suggested that entry of anions from aqueous solution into the capillary is associated with a decrease in free energy. DeFever et al.[136], performed MD simulations for removal of aromatic contaminants from water using graphene and GO surfaces. They elucidate the molecular interactions between naphthalene molecules play a significant role in enhancing their association with graphene and GO surface.

Graphene and GO for Separation of Organic Pollutants by External Pressure

Borges et al.[137] investigated the dynamics of water permeation in pristine graphene and GO membranes. Authors systematically analyzed the transport dynamics of the confined nanofluids depending on the interlayer distances and the role of the oxide functional groups under controlled thermodynamics conditions. They found that the water flux is much more effective for graphene than for graphene oxide membranes which is attributed to the hydrogen bonds formation between oxide functional groups and water, which traps the water molecules and prevents ultrafast water transport through the channels. Bong et al.[138] performed MD simulations with four different solvents, namely water, gasoline (consisting of heptane, octane, and hexyl benzene), kerosene (consisting of n-hexadecane and n-eicosane), and olive oil (consisting of palmitic acid, stearic acid, oleic acid, and linoleic acid) for selective filtration using graphene sheet grafted with different functional groups. The graphene sheet with high percentage coverage of hydroxyl and carboxylic functional groups blocks kerosene. Whereas water is not filtered out with low-percentage epoxide coverage. These results suggested that the surface functionalization of graphene sheet can solve particular separation problems involving oil and water mixtures. Bahamon et al.[139] studied to understanding the separation of phenol and ibuprofen from water using multilayered graphene oxide membranes. Results showed that 100% rejection organic solutes and greater water permeability inside GO membrane up to 20% than that in graphene layers, because of strong hydrogen-bonded interactions with the oxygenated groups. In a recent study conducted by Ansari et al.[140], the separation of perchlorates and trihalomethanes from aqueous solution using different functional groups (-F, -OH, and -H) placed on the edges of the GO nanopore was invested. It was found that functionalized GO nanosheet membrane showed high-water permeability, and perchlorate and trihalomethanes rejection passed through these pores.

Hou et al.[141] demonstrated that the permeation of liquid ethanol–water mixtures through a series of nanoporous graphene membranes with various pore sizes and shapes as shown in Figure 15a,c. The selective permeation of ethanol molecules across the graphene

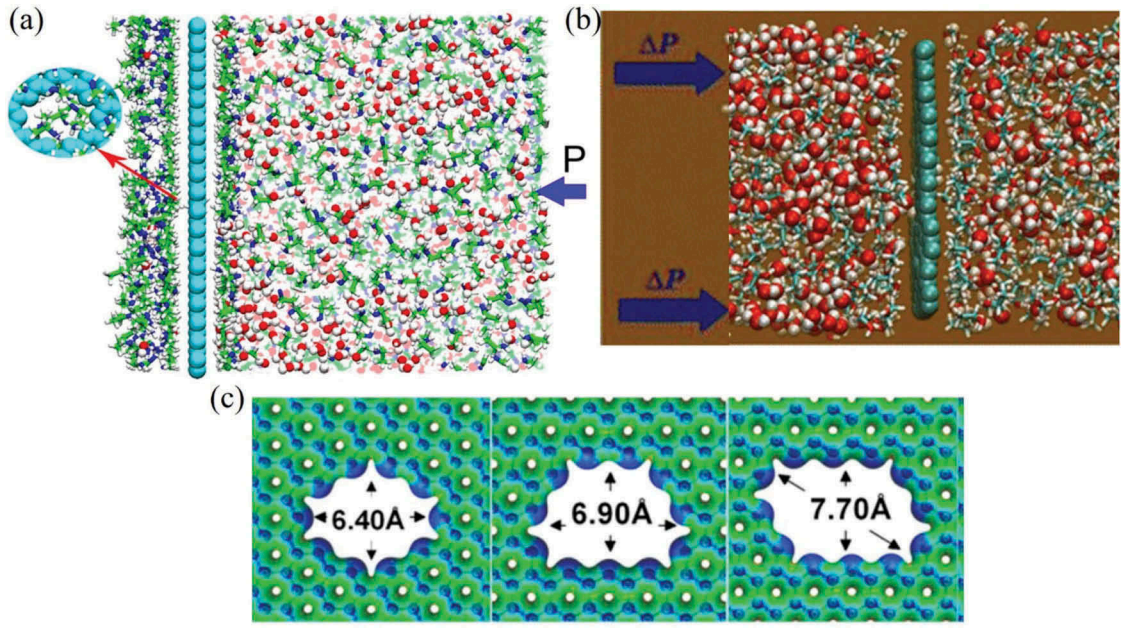

Figure 15. (a) The nonequilibrium permeation simulation system; the inset is the enlarged snapshot for ethanol molecules passing through the nanopore. Color cyan for nanoporous graphene; green, blue color represents the carbon, oxygen atoms of ethanol molecules; red and white color represents the oxygen and hydrogen atoms of water molecules. Adapted with permission from ref[141] Copyright (2016) American chemical society. (b) A snapshot of the molecular simulation system. Colors cyan, red, and white denotes for carbon, oxygen, and hydrogen atoms. Adapted with permission from ref[142] Copyright (2017) Springer Nature. (c) Pore structures and pore electron density isosurfaces of the nanoporous graphenes considered in the simulation. Adapted with permission from ref[141] Copyright (2016) American chemical society.

membranes is higher than water molecules. This result suggests that permeability of ethanol molecules shows several orders of magnitude higher than current pervaporation membranes. Shi et al.[142] presented ethanol/water separation using single-layer graphene with various pores and functional groups such as hydrophilic (–OH) and hydrophobic (–H) terminations. They found the separation performance of ethanol from water depends on the pore size, pore's chemistry, and applied hydrostatic pressure (see Fig. 15b). The hydrophilic functionalization of graphene nanopores is found to be more efficient for ethanol/water separation, due to

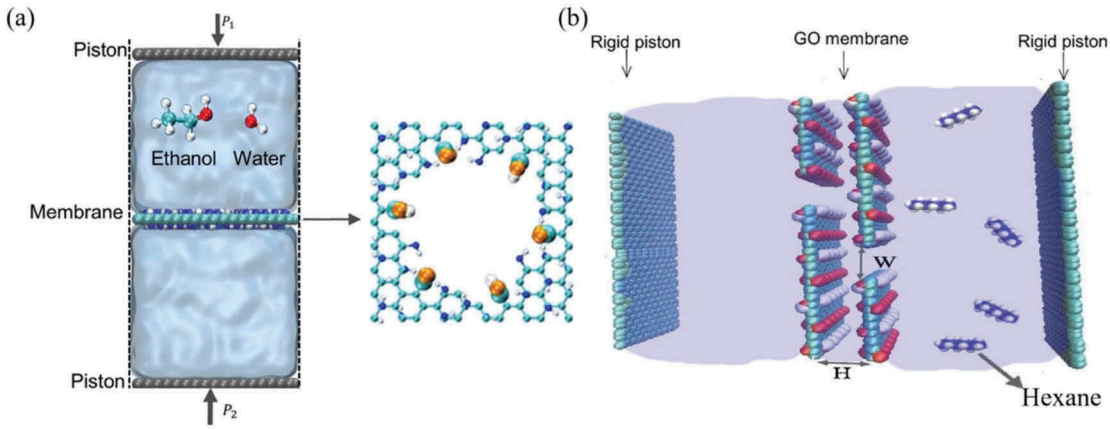

Figure 16. (a) The snapshot of molecular system for separation of water-ethanol by GO membrane having a single nanopore at its center, and six carbon atoms at the perimeter of its pore are functionalized using carboxyl groups. Zoom-in view of the nanopores in the GO membrane. The orange, blue, cyan, and white color denote the carboxyl oxygen, oxygen, carbon, and hydrogen atoms, respectively. Adapted with permission from ref[143] Copyright (2018) Elsevier. (b) A schematic illustration of the simulation system box of water-hexane separation by using GO membranes. Adapted with permission from ref[144] Copyright (2018) Elsevier.

lower energy barrier for water than the ethanol molecules in the pore vicinity compared to hydrophobic porous graphene membrane.

Similarly, Fang et al.[143], studied the separation of water and ethanol using single-layer GO sheets with different pore sizes and tuning the ionization of functional groups on the periphery of GO pores as shown in Figure 16a. They revealed that water to ethanol selectivity coefficient of ~7 within the pores of nominal diameter of 11.2Å and ionization of the COOH groups on the edge of the pores in the GO membranes. This improved the selectivity of water over ethanol molecules due to the ionization of the functional groups; the dominating factor is functional groups on the periphery of pores which enhances the accessibility of water molecules but suppresses the ethanol molecules at the same pores.

Recently, Foroutan et al.[144] investigated computationally the separation of water from a water-oil mixture by two-layer GO layers with varying interlayer spacing between two GO layers as well as gap size of GO (see Fig. 16b). Their results suggest that the reduction in the interlayer distance and size of the gap will decrease the permeability and flux of the water molecules, but the amount of water molecules separating from the oil increases. The GO functional groups also affect the water-oil separation, which is revealed by the hydrogen bonding calculations between GO and water molecules. The authors also calculated PMF to study the effect of functional groups on repelling oil molecules from the GO gaps. Yu et al.[145], studied the molecular permeation of ethanol-water mixtures passing through single-layer GO nanopores modified with COOH (carboxyl) and COO^- (ionized carboxyl) groups, respectively. They concluded that GO-COO^- pore showed a strong molecular affinity between water and COO^- group compared to the ethanol molecules, promoting the higher selective penetration of water relative to the ethanol. Liu et al.[146] explored the microstructure of GO membrane is optimized and the permeation behavior of water and ethanol through porous GO membranes with different pore sizes and O/C ratios. The adequately sized pore (D = 2.4 Å) and a high O/C ratio (R = 0.49) GO membrane attained the highest ethanol rejection and water flux.

Finally, we will end this section with a comparison of computational and experimental works. Until now, many experimental works[58,147–157] were conducted on the GO-based membranes for water purification. On the contrary, computational studies are very limited. There are some discrepancies among the simulation and experimental results which remain to be understood. The models in the computational studies mostly based on the ideal structures of graphene membranes, exhibiting a considerable discrepancy with the realistic structures in many aspects, such as the pore size and porosity in the NPG membranes, chemical modifications on pore edge and graphene surface both for the NPG and GO membranes, interlayer channel distance and topological structure in the GO membranes. However, the GO membrane areas in the simulations are usually on the order of square nanometers, which is many orders smaller than the real membrane area employed in the experiments. Though the simulations usually employed periodic boundary conditions, the complicated distributions of pores and channels in the GO membranes cannot be considered in the simulations with a small membrane area. The molecules (water, ion, etc.) involved in the simulations (range of hundreds and thousands) are very limited owing to the limitation of computation cost. The molecular permeance obtained by averaging the molecular transport rates in such short time periods may induce a non-negligible discrepancy with the experimentally measured data. One possible solution to solve the above-mentioned inadequacies would increase the length and time scales of molecular simulations by the means of coarse-grained method and other effective methods such as realistic topological structure, chemical composition, and quantum mechanical calculations. Such studies would be necessary for the translation of material realized in the lab scale to the industrial scale.

Summary and Future Scope of Work

This review highlighted the use of molecular simulation methods to study the removal of organic and inorganic pollutants from aqueous solutions using graphene and graphene-based materials by means of MD simulations. The simulation studies reveal that functionalized graphene and GO materials are a promising substitute of activated carbon and other materials that are presently used for desalination and purification of wastewater. The functionalized graphene and GO membranes possess higher water permeability that is several orders higher than the existing methods. The graphene and GO materials have been shown to have the potential to be one of the most reliable and versatile materials for wastewater treatment and have great potential for applications in environmental science. However, membrane affinity, molecular size, geometry confinement, and selective permeation are the key factors for designing more efficient graphene and GO membranes for separation of organic and inorganic pollutants from wastewater. Furthermore, the key challenge lies in understanding the synthesis

mechanism to produce a vigorous and cost-effectiveness membranes for practical applications. Although computational studies have shed light on transport mechanisms in idealized pores, an understanding of the structure and behavior of pores in real materials has only just started to emerge. Finally, additional research is needed to evaluate the cost-effectiveness of large-scale membrane fabrication, adsorption of multi-components, pilot-plant studies and monitoring of the long-term stability of membranes under practical application conditions. Significant work is needed to overcome these major challenges, for commercialization of graphene and GO materials for large-scale wastewater treatment. In this direction, molecular studies are highly desirable to provide essential information for the commercial application of graphene-based materials for desalinations and purification of wastewater.

Acknowledgments

This work is supported by Board of Research on Nuclear Sciences (BRNS), Department of Atomic Energy (DAE), and Government of India, sanctioned no.: 36(1)/14/02/2015-BRNS/100. We are grateful to HPC, IIT Kanpur for the computational support.

References

[1] Lubchenco, J. Entering the Century of the Environment: A New Social Contract for Science. *Science*. 1998, *279*(5350), 491–497. DOI: 10.1126/science.279.5350.491.

[2] Gavrilescu, M.; Demnerová, K.; Aamand, J.; Agathos, S; Fava, F. Emerging Pollutants in the Environment: Present and Future Challenges in Biomonitoring, Ecological Risks and Bioremediation. *New Biotechnol.* 2015, *32*(1), 147–156.

[3] Pal, A.; He, Y.; Jekel, M.; Reinhard, M.; Gin, K. Y.-H. Emerging Contaminants of Public Health Significance as Water Quality Indicator Compounds in the Urban Water Cycle. *Environ. Int.* 2014, *71*, 46–62. DOI: 10.1016/j.envint.2014.05.025.

[4] Fu, F.; Wang, Q. Removal of Heavy Metal Ions from Wastewaters: A Review. *J. Environ. Manage.* 2011, *92* (3), 407–418. DOI: 10.1016/j.jenvman.2010.11.011.

[5] Yilmaz, M.; Tay, T.; Kivanc, M.;Turk, H. Removal of copper(II) Ions from Aqueous Solution by a Lactic Acid Bacterium. *Braz. J. Chem. Eng.* 2010, *27*(2), 309–314.

[6] Xue, Z.; Cao, Y.; Liu, N.; Feng, L.; Jiang, L. Special Wettable Materials for Oil/water Separation. *J. Mater. Chem. A*. 2014, *2*(8), 2445–2460.

[7] Chandra, V.; Park, J.; Chun, Y.; Lee, J. W.; Hwang, I.-C.; Kim, K. S. Water-Dispersible Magnetite-Reduced Graphene Oxide Composites for Arsenic Removal. *ACS Nano*. 2010, *4*(7), 3979–3986.

[8] Tan, I. A. W.; Ahmad, A. L.; Hameed, B. H. Adsorption of Basic Dye on High-surface-area Activated Carbon Prepared from Coconut Husk: Equilibrium, Kinetic and Thermodynamic Studies. *J. Hazard. Mater.* 2008, *154*(1–3), 337–346. DOI: 10.1016/j.jhazmat.2007.10.031.

[9] Jacobson, M. Z. Review of Solutions to Global Warming, Air Pollution, and Energy Security. *Energy Environ. Sci.* 2009, *2*(2), 148–173. DOI: 10.1039/B809990C.

[10] Zhang, L.; Fang, M. Nanomaterials in Pollution Trace Detection and Environmental Improvement. *Nano Today*. 2010, *5*(2), 128–142. DOI: 10.1016/j.nantod.2010.03.002.

[11] El Qada, E. N.; Allen, S. J.; Walker, G. M. Adsorption of Basic Dyes from Aqueous Solution onto Activated Carbons. *Chem. Eng. J.* 2008, *135*(3), 174–184. DOI: 10.1016/j.cej.2007.02.023.

[12] Sulak, M. T.; Yatmaz, H. C. Removal of Textile Dyes from Aqueous Solutions with Eco-friendly Biosorbent. *Desalin. Water Treat.* 2012, *37*(1–3), 169–177. DOI: 10.1080/19443994.2012.661269.

[13] Zhang, H.; Feng, J.; Zhu, W.; Liu, C.; Xu, S.; Shao, P.; Wu, D.; Yang, W.; Gu, J. Chronic Toxicity of Rare-earth Elements on Human Beings. *Biol. Trace Elem. Res.* 2000, *73*(1), 1–17.

[14] Porru, S.; Placidi, D.; Quarta, C.; Sabbioni, E.; Pietra, R.; Fortaner, S. The Potential Role of Rare Earths in the Pathogenesis of Interstitial Lung Disease: A Case Report of Movie Projectionist as Investigated by Neutron Activation Analysis. *J. Trace Elem. Med. Biol.* 2001, *14*(4), 232–236.

[15] Zaichick, S.; Zaichick, V.; Karandashev, V.; Nosenko, S. Accumulation of Rare Earth Elements in Human Bone within the Lifespan. *Metallomics*. 2011, *3*(2), 186–194.

[16] Yoon, H. W.; Cho, Y. H.; Park, H. B. Graphene-based Membranes: Status and Prospects. *Phil. Trans. R. Soc. A*. 2016, *374*(2060), 20150024. DOI: 10.1098/rsta.2015.0024.

[17] Spiegler, K. S.; El-Sayed, Y. M. The Energetics of Desalination Processes. *Desalination*. 2001, *134*(1–3), 109–128. DOI: 10.1016/S0011-9164(01)00121-7.

[18] Greenlee, L. F.; Lawler, D. F.; Freeman, B. D.; Marrot, B; Moulin, P. Reverse Osmosis Desalination: Water Sources, Technology, and Today's Challenges. *Water Res.* 2009, *43*(9), 2317–2348.

[19] Zhu, A.; Rahardianto, A.; Christofides, P. D.; Cohen, Y. Reverse Osmosis Desalination with High Permeability Membranes — Cost Optimization and Research Needs. *Desalin. Water Treat.* 2010, *15*(1–3), 256–266.

[20] Elimelech, M.; Phillip, W. A. The Future of Seawater Desalination: Energy, Technology, and the Environment. *Science*. 2011, *333*(6043), 712–717. DOI: 10.1126/science.1200488.

[21] Huang, L.; Zhang, M.; Li, C.; Shi, G. Graphene-Based Membranes for Molecular Separation. *J. Phys. Chem. Lett.* 2015, *6*(14), 2806–2815.

[22] Lee, K. P.; Arnot, T. C.; Mattia, D. A Review of Reverse Osmosis Membrane Materials for desalination—Development to Date and Future Potential. *J. Membr. Sci.* 2011, 370(1–2), 1–22. DOI: 10.1016/j.memsci.2010.12.036.

[23] Humplik, T.; Lee, J.; O'Hern, S. C.; Fellman, B. A.; Baig, M. A.; Hassan, S. F.; Atieh, M. A.; Rahman, F.; Laoui, T.; Karnik, R.; et al. Nanostructured Materials for Water Desalination. *Nanotechnology*. 2011, *22*(29), 292001.

[24] Pendergast, M. M.; Hoek, E. M. V. A Review of Water Treatment Membrane Nanotechnologies. *Energy Environ. Sci.* 2011, *4*(6), 1946–1971. DOI: 10.1039/c0ee00541j.
[25] Mahmoud, K. A.; Mansoor, B.; Mansour, A.; Khraisheh, M. Functional Graphene Nanosheets: The Next Generation Membranes for Water Desalination. *Desalination*. 2015, *356*, 208–225. DOI: 10.1016/j.desal.2014.10.022.
[26] Hu, M.; Mi, B. Enabling Graphene Oxide Nanosheets as Water Separation Membranes. *Environ. Sci. Technol.* 2013, *47*(8), 3715–3723. DOI: 10.1021/es400571g.
[27] Misdan, N.; Lau, W. J.; Ismail, A. F. Seawater Reverse Osmosis (SWRO) Desalination by Thin-film Composite membrane—Current Development, Challenges and Future Prospects. *Desalination*. 2012, *287*, 228–237. DOI: 10.1016/j.desal.2011.11.001.
[28] Bernardo, P.; Drioli, E.; Golemme, G. Membrane Gas Separation: A Review/State of the Art. *Ind. Eng. Chem. Res.* 2009, *48*(10), 4638–4663. DOI: 10.1021/ie8019032.
[29] Gascon, J.; Kapteijn, F.; Zornoza, B.; Sebastián, V.; Casado, C.; Coronas, J. Practical Approach to Zeolitic Membranes and Coatings: State of the Art, Opportunities, Barriers, and Future Perspectives. *Chem. Mater.* 2012, *24*(15), 2829–2844.
[30] Dong, C.; Campell, A. S.; Eldawud, R.; Perhinschi, G.; Rojanasakul, Y.; Dinu, C. Z. Effects of Acid Treatment on Structure, Properties and Biocompatibility of Carbon Nanotubes. *Appl. Surf. Sci.* 2013, *264*, 261–268. DOI: 10.1016/j.apsusc.2012.09.180.
[31] Campbell, A. S.; Dong, C.; Dordick, J. S.; Dinu, C. Z. BioNano Engineered Hybrids for Hypochlorous Acid Generation. *Process Biochem.* 2013, *48*(9), 1355–1360.
[32] Kemnade, N.; Shearer, C. J.; Dieterle, D. J.; Cherevan, A. S.; Gebhardt, P.; Wilde, G.; Eder, D. Non-destructive Functionalisation for Atomic Layer Deposition of Metal Oxides on Carbon Nanotubes: Effect of Linking Agents and Defects. *Nanoscale*. 2015, *7*(7), 3028–3034.
[33] Baughman, R. H.; Zakhidov, A. A.; De Heer, W. A. Carbon Nanotubes – The Route toward Applications. *Science*. 2002, *297*(5582), 787–792. DOI: 10.1126/science.1060928.
[34] Yu, M.; Funke, H. H.; Falconer, J. L.; Noble, R. D. High Density, Vertically-Aligned Carbon Nanotube Membranes. *Nano Lett.* 2009, *9*(1), 225–229.
[35] Goh, P. S.; Ismail, A. F.; Ng, B. C. Carbon Nanotubes for Desalination: Performance Evaluation and Current Hurdles. *Desalination*. 2013, *308*, 2–14. DOI: 10.1016/j.desal.2012.07.040.
[36] Huang, H.; Ying, Y.; Peng, X. Graphene Oxide Nanosheet: An Emerging Star Material for Novel Separation Membranes. *J. Mater. Chem. A*. 2014, *2*(34), 13772–13782. DOI: 10.1039/C4TA02359E.
[37] Terrones, M.; Botello-Méndez, A. R.; Campos-Delgado, J.; López-Urías, F.; Vega-Cantú, Y. I.; Rodríguez-Macías, F. J.; Elías, A. L.; Muñoz-Sandoval, E.; Cano-Márquez, A. G.; Charlier, J.-C.; et al. Graphene and Graphite Nanoribbons: Morphology, Properties, Synthesis, Defects and Applications. *Nano Today*. 2010, *5*(4), 351–372.
[38] Chen, Y.; Zhang, B.; Liu, G.; Zhuang, X.; Kang, E.-T. Graphene and Its Derivatives: Switching ON and OFF. *Chem. Soc. Rev.* 2012, *41*(13), 4688–4707.
[39] Dikin, D. A.; Stankovich, S.; Zimney, E. J.; Piner, R. D.; Dommett, G. H. B.; Evmenenko, G.; Nguyen, S. T.; Ruoff, R. S. Preparation and Characterization of Graphene Oxide Paper. *Nature*. 2007, *448*(7152), 457–460.
[40] Paek, S.-M.; Yoo, E.; Honma, I. Enhanced Cyclic Performance and Lithium Storage Capacity of SnO2/Graphene Nanoporous Electrodes with Three-Dimensionally Delaminated Flexible Structure. *Nano Lett.* 2009, *9*(1), 72–75. DOI: 10.1021/nl802484w.
[41] Su, F.-Y.; You, C.; He, Y.-B.; Lv, W.; Cui, W.; Jin, F.; Li, B.; Yang, Q.-H.; Kang, F. Flexible and Planar Graphene Conductive Additives for Lithium-ion Batteries. *J. Mater. Chem.* 2010, *20*(43), 9644–9650.
[42] Yin, Z; Zhu, J; He, Q; Cao, X; Tan, C; Chen, H; Yan, Q; Zhang, H. Graphene-Based Materials for Solar Cell Applications. *Adv. Energy Mater.* 2013, *4*, 1300574.
[43] Tsetseris, L.; Pantelides, S. T. Graphene: An Impermeable or Selectively Permeable Membrane for Atomic Species? *Carbon*. 2014, *67*, 58–63. DOI: 10.1016/j.carbon.2013.09.055.
[44] Gai, J.-G.; Gong, X.-L.; Wang, -W.-W.; Zhang, X.; Kang, W.-L. An Ultrafast Water Transport Forward Osmosis Membrane: Porous Graphene. *J. Mater. Chem. A*. 2014, *2*(11), 4023–4028.
[45] Liu, H.; Dai, S.; Jiang, D. Permeance of H2 through Porous Graphene from Molecular Dynamics. *Solid State Commun.* 2013, *175–176*, 101–105. DOI: 10.1016/j.ssc.2013.07.004.
[46] You, Y.; Sahajwalla, V.; Yoshimura, M.; Joshi, R. K. Graphene and Graphene Oxide for Desalination. *Nanoscale*. 2015, *8*(1), 117–119.
[47] Jiang, D.; Cooper, V. R.; Dai, S. Porous Graphene as the Ultimate Membrane for Gas Separation. *Nano Lett.* 2009, *9*(12), 4019–4024. DOI: 10.1021/nl9021946.
[48] Cohen-Tanugi, D.; Grossman, J. C. Water Desalination across Nanoporous Graphene. *Nano Lett.* 2012, *12*(7), 3602–3608. DOI: 10.1021/nl3012853.
[49] Sint, K.; Wang, B.; Král, P. Selective Ion Passage through Functionalized Graphene Nanopores. *J. Am. Chem. Soc.* 2009, *131*(27), 9600. DOI: 10.1021/ja903655u.
[50] Konatham, D.; Yu, J.; Ho, T. A.; Striolo, A. Simulation Insights for Graphene-Based Water Desalination Membranes. *Langmuir*. 2013, *29*(38), 11884–11897.
[51] He, Z.; Zhou, J.; Lu, X.; Corry, B. Bioinspired Graphene Nanopores with Voltage-Tunable Ion Selectivity for Na + and K+. *ACS Nano*. 2013, *7*(11), 10148–10157.
[52] Owais, C.; James, A.; John, C.; Dhali, R.; Swathi, R. S. Selective Permeation through One-Atom-Thick Nanoporous Carbon Membranes: Theory Reveals Excellent Design Strategies! J. *Phys. Chem. B*. 2018, *122*(20), 5127–5146.
[53] Riyaz, M.; Goel, N. A QM/MM Study to Investigate Selectivity of Nanoporous Graphene Membrane for Arsenate and Chromate Removal from Water. *Chem. Phys. Lett.* 2017, *685*, 371–376. DOI: 10.1016/j.cplett.2017.08.005.
[54] Boukhvalov, D. W.; Katsnelson, M. I.; Son, Y.-W. Origin of Anomalous Water Permeation through Graphene Oxide Membrane. *Nano Lett.* 2013, *13*(8), 3930–3935. DOI: 10.1021/nl4020292.

[55] Boukhvalov, D. W.; Katsnelson, M. I. Modeling of Graphite Oxide. *J. Am. Chem. Soc.* 2008, *130*(32), 10697–10701. DOI: 10.1021/ja8021686.
[56] Wang, L.; Sun, Y. Y.; Lee, K.; West, D.; Chen, Z. F.; Zhao, J. J.; Zhang, S. B. Stability of Graphene Oxide Phases from First-principles Calculations. *Phys. Rev. B.* 2010, *82*(16), 161406.
[57] Joshi, R. K.; Carbone, P.; Wang, F. C.; Kravets, V. G.; Su, Y.; Grigorieva, I. V.; Wu, H. A.; Geim, A. K.; Nair, R. R. Precise and Ultrafast Molecular Sieving through Graphene Oxide Membranes. *Science*. 2014, *343*(6172), 752–754.
[58] Abraham, J.; Vasu, K. S.; Williams, C. D.; Gopinadhan, K.; Su, Y.; Cherian, C. T.; Dix, J.; Prestat, E.; Haigh, S. J.; Grigorieva, I. V.; et al. Tunable Sieving of Ions Using Graphene Oxide Membranes. *Nat. Nanotechnol.* 2017, *12*(6), 546–550.
[59] Wei, N.; Peng, X.; Xu, Z. Understanding Water Permeation in Graphene Oxide Membranes. *ACS Appl. Mater. Interfaces.* 2014, *6*(8), 5877–5883. DOI: 10.1021/am500777b.
[60] Guerrero-Avilés, R.; Orellana, W. Energetics and Diffusion of Liquid Water and Hydrated Ions through Nanopores in Graphene: Ab Initio Molecular Dynamics Simulation. *Phys. Chem. Chem. Phys.* 2017, *19*(31), 20551–20558. DOI: 10.1039/C7CP03449K.
[61] Heath, J. J.; Kuroda, M. A. First Principles Studies of the Interactions between Alkali Metal Elements and Oxygen-passivated Nanopores in Graphene. *Phys. Chem. Chem. Phys.* 2018, *20*(40), 25822–25828. DOI: 10.1039/C8CP04958K.
[62] Wang, Y.; He, Z.; Gupta, K. M.; Shi, Q.; Lu, R. Molecular Dynamics Study on Water Desalination through Functionalized Nanoporous Graphene. *Carbon*. 2017, *116*, 120–127. DOI: 10.1016/j.carbon.2017.01.099.
[63] Gai, J.-G.; Gong, X.-L. Zero Internal Concentration Polarization FO Membrane: Functionalized Graphene. *J. Mater. Chem. A*. 2013, *2*(2), 425–429. DOI: 10.1039/C3TA13562D.
[64] Ang, E. Y. M.; Ng, T. Y.; Yeo, J.; Liu, Z.; Geethalakshmi, K. R. Free-standing Graphene Slit Membrane for Enhanced Desalination. *Carbon*. 2016, *110*, 350–355. DOI: 10.1016/j.carbon.2016.09.043.
[65] Muscatello, J.; Jaeger, F.; Matar, O. K.; Müller, E. A. Optimizing Water Transport through Graphene-Based Membranes: Insights from Nonequilibrium Molecular Dynamics. *ACS Appl. Mater. Interfaces.* 2016, *8*(19), 12330–12336.
[66] Kommu, A.; Namsani, S.; Singh, J. K. Removal of Heavy Metal Ions Using Functionalized Graphene Membranes: A Molecular Dynamics Study. *RSC Adv.* 2016, *6*(68), 63190–63199. DOI: 10.1039/C6RA06817K.
[67] Barakat, M. A. New Trends in Removing Heavy Metals from Industrial Wastewater. *Arabian J. Chem.* 2011, *4*(4), 361–377. DOI: 10.1016/j.arabjc.2010.07.019.
[68] Li, Y.; Xu, Z.; Liu, S.; Zhang, J.; Yang, X. Molecular Simulation of Reverse Osmosis for Heavy Metal Ions Using Functionalized Nanoporous Graphenes. *Comput. Mater. Sci.* 2017, *139*, 65–74. DOI: 10.1016/j.commatsci.2017.07.032.
[69] Chen, Q.; Yang, X. Pyridinic Nitrogen Doped Nanoporous Graphene as Desalination Membrane: Molecular Simulation Study. *J. Membr. Sci.* 2015, *496*, 108–117. DOI: 10.1016/j.memsci.2015.08.052.
[70] Qiu, Y.; Schwegler, B. R.; Wang, L.-P. Polarizable Molecular Simulations Reveal How Silicon-Containing Functional Groups Govern the Desalination Mechanism in Nanoporous Graphene. *J. Chem. Theory Comput.* 2018, 14(8), 4279–4290. DOI: 10.1021/acs.jctc.8b00226.
[71] Köhler, M. H.; Bordin, J. R.; Barbosa, M. C. Ion Flocculation in Water: From Bulk to Nanoporous Membrane Desalination. *J. Mol. Liq.* 2019, *277*, 516–521. DOI: 10.1016/j.molliq.2018.12.077.
[72] Chogani, A.; Moosavi, A.; Bagheri Sarvestani, A.; Shariat, M. The Effect of Chemical Functional Groups and Salt Concentration on Performance of Single-layer Graphene Membrane in Water Desalination Process: A Molecular Dynamics Simulation Study. *J. Mol. Liq.* 2020, *301*, 112478. DOI: 10.1016/j.molliq.2020.112478.
[73] Surwade, S. P.; Smirnov, S. N.; Vlassiouk, I. V.; Unocic, R. R.; Veith, G. M.; Dai, S.; Mahurin, S. M. Water Desalination Using Nanoporous Single-layer Graphene. *Nat. Nanotechnol.* 2015, *10*(5), 459–464.
[74] Kazemi, A. S.; Hosseini, S. M.; Abdi, Y. Large Total Area Membrane of Suspended Single Layer Graphene for Water Desalination. *Desalination*. 2019, *451*, 160–171. DOI: 10.1016/j.desal.2017.12.050.
[75] Qin, Y.; Hu, Y.; Koehler, S.; Cai, L.; Wen, J.; Tan, X.; Xu, W. L.; Sheng, Q.; Hou, X.; Xue, J.; et al. Ultrafast Nanofiltration through Large-Area Single-Layered Graphene Membranes. *ACS Appl. Mater. Interfaces.* 2017, *9*(11), 9239–9244.
[76] Wang, L.; Boutilier, M. S. H.; Kidambi, P. R.; Jang, D.; Hadjiconstantinou, N. G.; Karnik, R. Fundamental Transport Mechanisms, Fabrication and Potential Applications of Nanoporous Atomically Thin Membranes. *Nat. Nanotechnol.* 2017, *12*(6), 509–522.
[77] Cohen-Tanugi, D.; Lin, L.-C.; Grossman, J. C. Multilayer Nanoporous Graphene Membranes for Water Desalination. *Nano Lett.* 2016, *16*(2), 1027–1033. DOI: 10.1021/acs.nanolett.5b04089.
[78] Yoshida, H.; Bocquet, L. Labyrinthine Water Flow across Multilayer Graphene-based Membranes: Molecular Dynamics versus Continuum Predictions. *J. Chem. Phys.* 2016, *144*(23), 234701. DOI: 10.1063/1.4953685.
[79] Dahanayaka, M.; Liu, B.; Hu, Z.; Pei, Q.-X.; Chen, Z.; Law, A. W.-K.; Zhou, K. Graphene Membranes with Nanoslits for Seawater Desalination via Forward Osmosis. *Phys. Chem. Chem. Phys.* 2017, *19*(45), 30551–30561.
[80] Celebi, K.; Buchheim, J.; Wyss, R. M.; Droudian, A.; Gasser, P.; Shorubalko, I.; Kye, J.-I.; Lee, C.; Park, H. G. Ultimate Permeation Across Atomically Thin Porous Graphene. *Science*. 2014, *344*(6181), 289.
[81] Kargar, M.; Lohrasebi, A. Water Flow Modeling through a Graphene-based Nanochannel: Theory and Simulation. *Phys. Chem. Chem. Phys.* 2019, *21*(6), 3304–3309. DOI: 10.1039/C8CP06839A.
[82] Sahu, P.; Ali, S. Breakdown of Continuum Model for Water Transport and Desalination through Ultrathin Graphene Nanopores: Insights from Molecular Dynamics Simulations. *Phys. Chem. Chem. Phys.*

2019, *21*(38), 21389–21406. DOI: 10.1039/C9CP04364K.
[83] Seo, D. H.; Pineda, S.; Woo, Y. C.; Xie, M.; Murdock, A. T.; Ang, E. Y. M.; Jiao, Y.; Park, M. J.; Lim, S. I.; Lawn, M.; et al. Anti-fouling Graphene-based Membranes for Effective Water Desalination. *Nat. Commun.* 2018, *9*(1), 683.
[84] Nicolaï, A.; Sumpter, B. G.; Meunier, V. Tunable Water Desalination across Graphene Oxide Framework Membranes. *Phys. Chem. Chem. Phys.* 2014, *16*(18), 8646–8654. DOI: 10.1039/c4cp01051e.
[85] Chen, B.; Jiang, H.; Liu, X.; Hu, X. Molecular Insight into Water Desalination across Multilayer Graphene Oxide Membranes. *ACS Appl. Mater. Interfaces.* 2017, *9*(27), 22826–22836.
[86] Dai, H.; Xu, Z.; Yang, X. Water Permeation and Ion Rejection in Layer-by-Layer Stacked Graphene Oxide Nanochannels: A Molecular Dynamics Simulation. *J. Phys. Chem. C.* 2016, *120*(39), 22585–22596. DOI: 10.1021/acs.jpcc.6b05337.
[87] Devanathan, R.; Chase-Woods, D.; Shin, Y.; Gotthold, D. W. Molecular Dynamics Simulations Reveal that Water Diffusion between Graphene Oxide Layers Is Slow. *Sci. Rep.* 2016, *6*(1), 29484.
[88] Willcox, J. A. L.; Kim, H. J. Molecular Dynamics Study of Water Flow across Multiple Layers of Pristine, Oxidized, and Mixed Regions of Graphene Oxide. *ACS Nano*. 2017, *11*(2), 2187–2193. DOI: 10.1021/acsnano.6b08538.
[89] Cohen-Tanugi, D.; Grossman, J. C. Water Permeability of Nanoporous Graphene at Realistic Pressures for Reverse Osmosis Desalination. *J. Chem. Phys.* 2014, *141*(7), 074704. DOI: 10.1063/1.4892638.
[90] Fang, C.; Yu, Z.; Qiao, R. Impact of Surface Ionization on Water Transport and Salt Leakage through Graphene Oxide Membranes. *J. Phys. Chem. C.* 2017, *121*(24), 13412–13420. DOI: 10.1021/acs.jpcc.7b04283.
[91] Hosseini, M.; Azamat, J.; Erfan-Niya, H. Improving the Performance of Water Desalination through Ultra-permeable Functionalized Nanoporous Graphene Oxide Membrane. *Appl. Surf. Sci.* 2018, *427*, 1000–1008. DOI: 10.1016/j.apsusc.2017.09.071.
[92] Gogoi, A.; Konch, T. J.; Raidongia, K.; Anki Reddy, K. Water and Salt Dynamics in Multilayer Graphene Oxide (GO) Membrane: Role of Lateral Sheet Dimensions. *J. Membr. Sci.* 2018, *563*, 785–793. DOI: 10.1016/j.memsci.2018.06.031.
[93] Giri, A. K.; Teixeira, F.; Cordeiro, M. N. D. S. Salt Separation from Water Using Graphene Oxide Nanochannels: A Molecular Dynamics Simulation Study. *Desalination*. 2019, *460*, 1–14. DOI: 10.1016/j.desal.2019.02.014.
[94] Lohrasebi, A.; Koslowski, T. Modeling Water Purification by an Aquaporin-inspired Graphene-based Nano-channel. *J. Mol. Model.* 2019, *25*(9), 280. DOI: 10.1007/s00894-019-4160-y.
[95] Qiu, R.; Xiao, J.; Chen, X. D.; Selomulya, C.; Zhang, X.; Woo, M. W. Relationship between Desalination Performance of Graphene Oxide Membranes and Edge Functional Groups. *ACS Appl. Mater. Interfaces.* 2020, *12*(4), 4769–4776.
[96] Li, W.; Zhang, L.; Zhang, X.; Zhang, M.; Liu, T.; Chen, S. Atomic Insight into Water and Ion Transport in 2D Interlayer Nanochannels of Graphene Oxide Membranes: Implication for Desalination. *J. Membr. Sci.* 2020, *596*, 117744. DOI: 10.1016/j.memsci.2019.117744.
[97] Azamat, J. Functionalized Graphene Nanosheet as a Membrane for Water Desalination Using Applied Electric Fields: Insights from Molecular Dynamics Simulations. *J. Phys. Chem. C.* 2016, *120*(41), 23883–23891. DOI: 10.1021/acs.jpcc.6b08481.
[98] Rollings, R. C.; Kuan, A. T.; Golovchenko, J. A. Ion Selectivity of Graphene Nanopores. *Nat. Commun.* 2016, *7*(1), 11408. DOI: 10.1038/ncomms11408.
[99] Ruan, Y.; Zhu, Y.; Zhang, Y.; Gao, Q.; Lu, X.; Lu, L. Molecular Dynamics Study of Mg2+/Li+ Separation via Biomimetic Graphene-Based Nanopores: The Role of Dehydration in Second Shell. *Langmuir*. 2016, *32*(51), 13778–13786.
[100] Zhu, Y.; Ruan, Y.; Zhang, Y.; Chen, Y.; Lu, X.; Lu, L. Mg2+-Channel-Inspired Nanopores for Mg2+/Li+ Separation: The Effect of Coordination on the Ionic Hydration Microstructures. *Langmuir*. 2017, *33*(36), 9201–9210.
[101] Nguyen, C. T.; Beskok, A. Saltwater Transport through Pristine and Positively Charged Graphene Membranes. *J. Chem. Phys.* 2018, *149*(2), 024704. DOI: 10.1063/1.5032207.
[102] Nguyen, C. T.; Beskok, A. Charged Nanoporous Graphene Membranes for Water Desalination. *Phys. Chem. Chem. Phys.* 2019, *21*(18), 9483–9494. DOI: 10.1039/C9CP01079C.
[103] Zhang, H.; Liu, B.; Wu, M.-S.; Zhou, K.; Law, A. W.-K. Transport of Salty Water through Graphene Bilayer in an Electric Field: A Molecular Dynamics Study. *Comput. Mater. Sci.* 2017, *131*, 100–107. DOI: 10.1016/j.commatsci.2017.01.039.
[104] Lohrasebi, A.; Rikhtehgaran, S. Ion Separation and Water Purification by Applying External Electric Field on Porous Graphene Membrane. *Nano Res.* 2018, *11*(4), 2229–2236. DOI: 10.1007/s12274-017-1842-6.
[105] Anitha, K.; Namsani, S.; Singh, J. K. Removal of Heavy Metal Ions Using a Functionalized Single-walled Carbon Nanotube: A Molecular Dynamics Study. *J. Phys. Chem. A*. 2015, *119*(30), 8349–8358. DOI: 10.1021/acs.jpca.5b03352.
[106] Tomalia, D. A.; Baker, H.; Dewald, J.; Hall, M.; Kallos, G.; Martin, S.; Roeck, J.; Ryder, J.; Smith, P. A New Class of Polymers: Starburst-Dendritic Macromolecules. *Polym. J.* 1985, *17*(1), 117.
[107] Tomalia, D. A.; Baker, H.; Dewald, J.; Hall, M.; Kallos, G.; Martin, S.; Roeck, J.; Ryder, J.; Smith, P. Dendritic Macromolecules: Synthesis of Starburst Dendrimers. *Macromolecules*. 1986, *19*(9), 2466–2468.
[108] Yuan, Y.; Zhang, G.; Li, Y.; Zhang, G.; Zhang, F.; Fan, X. Poly(amidoamine) Modified Graphene Oxide as an Efficient Adsorbent for Heavy Metal Ions. *Polym. Chem.* 2013, *4*(6), 2164–2167.
[109] Zhang, F.; Wang, B.; He, S.; Man, R. Preparation of Graphene-Oxide/Polyamidoamine Dendrimers and Their Adsorption Properties toward Some Heavy

Metal Ions. *J. Chem. Eng. Data*. 2014, *59*(5), 1719–1726.
[110] Kommu, A.; Velachi, V.; Cordeiro, M. N. D.; Singh, J. K. Removal of Pb (II) Ion Using PAMAM Dendrimer Grafted Graphene and Graphene Oxide Surfaces: A Molecular Dynamics Study. *J. Phys. Chem. A*. 2017, *121*(48), 9320–9329.
[111] Bayat, A.; Aghamiri, S. F.; Moheb, A.; Vakili-Nezhaad, G. R. Oil Spill Cleanup from Sea Water by Sorbent Materials. *Chem. Eng. Technol.* 2005, *28*(12), 1525–1528.
[112] Adebajo, M. O.; Frost, R. L.; Kloprogge, J. T.; Carmody, O.; Kokot, S. Porous Materials for Oil Spill Cleanup: A Review of Synthesis and Absorbing Properties. *J. Porous Mater.* 2003, *10*(3), 159–170.
[113] Deschamps, G.; Caruel, H.; Borredon, M.-E.; Bonnin, C.; Vignoles, C. Oil Removal from Water by Selective Sorption on Hydrophobic Cotton Fibers. 1. Study of Sorption Properties and Comparison with Other Cotton Fiber-Based Sorbents. *Environ. Sci. Technol.* 2003, *37*(5), 1013–1015.
[114] Sohn, K.; Na, Y. J.; Chang, H.; Roh, K.-M.; Dong Jang, H.; Huang, J. Oil Absorbing Graphene Capsules by Capillary Molding. *Chem. Commun.* 2012, *48*(48), 5968–5970.
[115] Thanikaivelan, P.; Narayanan, N. T.; Pradhan, B. K.; Ajayan, P. M. Collagen Based Magnetic Nanocomposites for Oil Removal Applications. *Sci. Rep.* [Internet]. 2012, 2. https://www.ncbi.nlm.nih.gov/pmc/articles/PMC3262048/ (accessed Mar 31, 2018).
[116] Zhu, Q.; Pan, Q.; Liu, F. Facile Removal and Collection of Oils from Water Surfaces through Superhydrophobic and Superoleophilic Sponges. *J. Phys. Chem. C.* 2011, *115*(35), 17464–17470. DOI: 10.1021/jp2043027.
[117] Calcagnile, P.; Fragouli, D.; Bayer, I. S.; Anyfantis, G. C.; Martiradonna, L.; Cozzoli, P. D.; Cingolani, R.; Athanassiou, A. Magnetically Driven Floating Foams for the Removal of Oil Contaminants from Water. *ACS Nano*. 2012, *6*(6), 5413–5419.
[118] Yuan, J.; Liu, X.; Akbulut, O.; Hu, J.; Suib, S. L.; Kong, J.; Stellacci, F. Superwetting Nanowire Membranes for Selective Absorption. *Nat. Nanotechnol.* 2008, *3*(6), 332–336.
[119] Cong, H.-P.; Ren, X.-C.; Wang, P.; Yu, S.-H. Macroscopic Multifunctional Graphene-Based Hydrogels and Aerogels by a Metal Ion Induced Self-Assembly Process. *ACS Nano*. 2012, *6*(3), 2693–2703.
[120] Chen, S.-H.; Yu, K.-C.; Lin, -S.-S.; Chang, D.-J.; Liou, R. M. Pervaporation Separation of Water/ethanol Mixture by Sulfonated Polysulfone Membrane. *J. Membr. Sci.* 2001, *183*(1), 29–36.
[121] Azamat, J.; Khataee, A.; Joo, S. W. Molecular Dynamics Simulation of Trihalomethanes Separation from Water by Functionalized Nanoporous Graphene under Induced Pressure. *Chem. Eng. Sci.* 2015, *127*, 285–292. DOI: 10.1016/j.ces.2015.01.048.
[122] Zhao, M.; Yang, X. Segregation Structures and Miscellaneous Diffusions for Ethanol/Water Mixtures in Graphene-Based Nanoscale Pores. *J. Phys. Chem. C.* 2015, *119*(37), 21664–21673. DOI: 10.1021/acs.jpcc.5b03307.
[123] Kommu, A.; Singh, J. K. Separation of Ethanol and Water Using Graphene and Hexagonal Boron Nitride Slit Pores: A Molecular Dynamics Study. *J. Phys. Chem. C.* 2017, *121*(14), 7867–7880. DOI: 10.1021/acs.jpcc.7b00172.
[124] Gao, Q.; Zhu, Y.; Ruan, Y.; Zhang, Y.; Zhu, W.; Lu, X.; Lu, L. Effect of Adsorbed Alcohol Layers on the Behavior of Water Molecules Confined in A Graphene Nanoslit: A Molecular Dynamics Study. *Langmuir*. 2017, *33*(42), 11467–11474.
[125] Borthakur, P.; Boruah, P. K.; Hussain, N.; Sharma, B.; Das, M. R.; Matić, S.; Řeha, D.; Minofar, B. Experimental and Molecular Dynamics Simulation Study of Specific Ion Effect on the Graphene Oxide Surface and Investigation of the Influence on Reactive Extraction of Model Dye Molecule at Water–Organic Interface. *J. Phys. Chem. C.* 2016, *120*(26), 14088–14100.
[126] Hou, D.; Zhang, Q.; Wang, M.; Zhang, J.; Wang, P.; Ge, Y. Molecular Dynamics Study Onwater and Ions on the Surface of Graphene Oxide Sheet: Effects of Functional Groups. *Comput. Mater. Sci.* 2019, *167*, 237–247. DOI: 10.1016/j.commatsci.2019.05.038.
[127] Wang, X.; Liu, Y.; Xu, J.; Li, S.; Zhang, F.; Ye, Q.; Zhai, X.; Zhao, X. Molecular dynamics study of stability and diffusion of graphene-based drug delivery systems. J. Nanomater. 2015 doi:10.1155/2015/872079
[128] Mahdavi, M.; Rahmani, F.; Nouranian, S. Molecular Simulation of pH-dependent Diffusion, Loading, and Release of Doxorubicin in Graphene and Graphene Oxide Drug Delivery Systems. *J. Mater. Chem. B.* 2016, *4*(46), 7441–7451. DOI: 10.1039/C6TB00746E.
[129] Safdari, F.; Raissi, H.; Shahabi, M.; Zaboli, M. DFT Calculations and Molecular Dynamics Simulation Study on the Adsorption of 5-Fluorouracil Anticancer Drug on Graphene Oxide Nanosheet as a Drug Delivery Vehicle. *J. Inorg. Organomet. Polym.* 2017, *27*(3), 805–817.
[130] Hasanzade, Z.; Raissi, H. Density Functional Theory Calculations and Molecular Dynamics Simulations of the Adsorption of Ellipticine Anticancer Drug on Graphene Oxide Surface in Aqueous Medium as Well as under Controlled pH Conditions. *J. Mol. Liq.* 2018, *255*, 269–278. DOI: 10.1016/j.molliq.2018.01.159.
[131] Tang, H.; Zhao, Y.; Shan, S.; Yang, X.; Liu, D.; Cui F.; Xing B. Theoretical Insight into the Adsorption of Aromatic Compounds on Graphene Oxide. *Environ. Sci.* 2018, *5*, 2357–2367.
[132] You, X.; He, M.; Cao, X.; Wang, P.; Wang, J.; Li, L. Molecular Dynamics Simulations of Removal of Nonylphenol Pollutants by Graphene Oxide: Experimental Study and Modelling. *Appl. Surf. Sci.* 2019, *475*, 621–626. DOI: 10.1016/j.apsusc.2019.01.006.
[133] Chang, S.; Zhang, Q.; Lu, Y.; Wu, S.; Wang, W. High-efficiency and Selective Adsorption of Organic Pollutants by Magnetic CoFe2O4/graphene Oxide Adsorbents: Experimental and Molecular Dynamics Simulation Study. *Sep. Purif. Technol.* 2020, *238*, 116400. DOI: 10.1016/j.seppur.2019.116400.

[134] Liu, J.; Li, P.; Xiao, H.; Zhang, Y.; Shi, X.; Lü, X.; Chen, X. Understanding Flocculation Mechanism of Graphene Oxide for Organic Dyes from Water: Experimental and Molecular Dynamics Simulation. *AIP Adv.* 2015, *5*(11), 117151.

[135] Williams, C. D.; Carbone, P. Selective Removal of Technetium from Water Using Graphene Oxide Membranes. *Environ. Sci. Technol.* 2016, *50*(7), 3875–3881. DOI: 10.1021/acs.est.5b06032.

[136] DeFever, R. S.; Geitner, N. K.; Bhattacharya, P.; Ding, F.; Ke, P. C.; Sarupria, S. PAMAM Dendrimers and Graphene: Materials for Removing Aromatic Contaminants from Water. *Environ. Sci. Technol.* 2015, *49*(7), 4490–4497.

[137] Borges, D. D.; Woellner, C. F.; Autreto, P. A. S.; Galvao, D. S. Water/Alcohol Separation in Graphene Oxide Membranes: Insights from Molecular Dynamics and Monte Carlo Simulations. *MRS Advances.* 2018, *3* (1–2), 109–114.

[138] Bong, J.; Lim, T.; Seo, K.; Kwon, C.-A.; Park, J. H.; Kwak, S. K.; Ju, S. Dynamic Graphene Filters for Selective Gas-water-oil Separation. *Sci. Rep.* 2015, *5*(1), 14321.

[139] Bahamon, D.; Vega, L. F. Molecular Simulations of Phenol and Ibuprofen Removal from Water Using Multilayered Graphene Oxide Membranes. *Mol. Phys.* 2019, 117(23–24), 3703–3714. DOI: 10.1080/00268976.2019.1662129.

[140] Ansari, P.; Azamat, J.; Khataee, A. Separation of Perchlorates from Aqueous Solution Using Functionalized Graphene Oxide Nanosheets: A Computational Study. *J. Mater. Sci.* 2019, *54*(3), 2289–2299. DOI: 10.1007/s10853-018-3045-2.

[141] Hou, Y.; Xu, Z.; Yang, X. Interface-Induced Affinity Sieving in Nanoporous Graphenes for Liquid-Phase Mixtures. *J. Phys. Chem. C.* 2016, *120*(7), 4053–4060. DOI: 10.1021/acs.jpcc.5b10287.

[142] Shi, Q.; He, Z.; Gupta, K. M.; Wang, Y.; Lu, R. Efficient Ethanol/water Separation via Functionalized Nanoporous Graphene Membranes: Insights from Molecular Dynamics Study. *J. Mater. Sci.* 2017, *52*(1), 173–184.

[143] Fang, C.; Wu, H.; Lee, S.-Y.; Mahajan, R. L.; Qiao, R. The Ionized Graphene Oxide Membranes for Water-ethanol Separation. *Carbon.* 2018, *136*, 262–269. DOI: 10.1016/j.carbon.2018.04.077.

[144] Foroutan, M.; Zahedi, H.; Soleimani, E. Investigation of Water-oil Separation via Graphene Oxide Membranes: A Molecular Dynamics Study. *Colloids Surf. A.* 2018, *555*, 201–208. DOI: 10.1016/j.colsurfa.2018.07.002.

[145] Yu, T.; Xu, Z.; Liu, S.; Liu, H.; Yang, X. Enhanced Hydrophilicity and Water-permeating of Functionalized Graphene-oxide Nanopores: Molecular Dynamics Simulations. *J. Membr. Sci.* 2018, *550*, 510–517. DOI: 10.1016/j.memsci.2017.10.060.

[146] Liu, Q.; Wu, Y.; Wang, X.; Liu, G.; Zhu, Y.; Tu, Y.; Lu, X.; Jin, W. Molecular Dynamics Simulation of Water-ethanol Separation through Monolayer Graphene Oxide Membranes: Significant Role of O/C Ratio and Pore Size. *Sep. Purif. Technol.* 2019, *224*, 219–226. DOI: 10.1016/j.seppur.2019.05.030.

[147] Li, W.; Wu, W.; Li, Z. Controlling Interlayer Spacing of Graphene Oxide Membranes by External Pressure Regulation. *ACS Nano.* 2018, *12*(9), 9309–9317. DOI: 10.1021/acsnano.8b04187.

[148] Zhou, K.-G.; Vasu, K. S.; Cherian, C. T.; Neek-Amal, M.; Zhang, J. C.; Ghorbanfekr-Kalashami, H.; Huang, K.; Marshall, O. P.; Kravets, V. G.; Abraham, J.; et al. Electrically Controlled Water Permeation through Graphene Oxide Membranes. *Nature.* 2018, *559*(7713), 236–240.

[149] Ying, Y.; Ying, W.; Guo, Y.; Peng, X. Cross-flow-assembled Ultrathin and Robust Graphene Oxide Membranes for Efficient Molecule Separation. *Nanotechnology.* 2018, *29*(15), 155602.

[150] Thebo, K. H.; Qian, X.; Zhang, Q.; Chen, L.; Cheng, H.-M.; Ren, W. Highly Stable Graphene-oxide-based Membranes with Superior Permeability. *Nat. Commun.* 2018, *9*(1), 1486.

[151] Lee, C. S.; Choi, M.; Hwang, Y. Y.; Kim, H.; Kim, M. K.; Lee, Y. J. Facilitated Water Transport through Graphene Oxide Membranes Functionalized with Aquaporin-Mimicking Peptides. *Adv.Mate.* 2018, *30*(14), 1705944.

[152] Xu, W. L.; Fang, C.; Zhou, F.; Song, Z.; Liu, Q.; Qiao, R.; Yu, M. Self-Assembly: A Facile Way of Forming Ultrathin, High-Performance Graphene Oxide Membranes for Water Purification. *Nano Lett.* 2017, *17*(5), 2928–2933.

[153] Liu, H.; Wang, H.; Zhang, X. Facile Fabrication of Freestanding Ultrathin Reduced Graphene Oxide Membranes for Water Purification. *Adv.Mate.* 2015, *27*(2), 249–254. DOI: 10.1002/adma.v27.2.

[154] Huang, L.; Li, Y.; Zhou, Q.; Yuan, W.; Shi, G. Graphene Oxide Membranes with Tunable Semipermeability in Organic Solvents. *Adv.Mate.* 2015, *27*(25), 3797–3802.

[155] Tang, Y. P.; Paul, D. R.; Chung, T. S. Free-standing Graphene Oxide Thin Films Assembled by a Pressurized Ultrafiltration Method for Dehydration of Ethanol. *J. Membr. Sci.* 2014, *458*, 199–208. DOI: 10.1016/j.memsci.2014.01.062.

[156] Li, B.; Cui, Y.; Japip, S.; Thong, Z.; Chung, T.-S. Graphene Oxide (GO) Laminar Membranes for Concentrating Pharmaceuticals and Food Additives in Organic Solvents. *Carbon.* 2018, *130*, 503–514. DOI: 10.1016/j.carbon.2018.01.040.

[157] Tang, Y. P.; Chan, J. X.; Chung, T. S.; Weber, M.; Staudt, C.; Maletzko, C. Simultaneously Covalent and Ionic Bridging Towards Antifouling of GO-imbedded Nanocomposite Hollow Fiber Membranes. *J. Mater. Chem. A.* 2015, *3*(19), 10573–10584.